RECENT PRACTICE AND RESEARCH OF GEOSYNTHETIC-REINFORCED EARTH STRUCTURES IN JAPAN

Fumio Tatsuoka[1]

ABSTRACT

The construction of permanent geosynthetic-reinforced soil (GRS) retaining walls (RWs) with a full-height rigid facing for railways, including high-speed train lines, and also highways started about twenty years ago in Japan. The total length of this type of GRS RW is now more than 100 km, replacing traditional cantilever reinforced concrete RWs and steel-reinforced soil RWs. Although most of the new type GRS RWs are new walls, many were also constructed replacing traditional type RWs and embankments that collapsed during recent earthquakes and heavy rainfalls. Several case histories typical of the newly constructed GRS RWs and those constructed to replace collapsed traditional type RWs and embankments are presented. By taking advantages of this technology, a number of bridge abutments with geosynthetic-reinforced backfill were constructed. The latest version, called the GRS integral bridge, comprises a continuous girder integrated to a pair of RC facing with the backfill reinforced with geosynthetic reinforcement layers firmly connected to the back of the facing. Results from static and dynamic model tests that show advantages of the GRS integral bridge are presented.

Key words: Bridge abutment, geosynthetics, model tests, reinforced earth, retaining walls, integral bridge.

1. INTRODUCTION

Construction of geosynthetic-reinforced soil retaining walls (GRS RWs) and geosynthetic-reinforced steep-sloped embankments has become popular these two decades in Japan, following pioneering works in Europe and the North America. Among those used in Japan, a couple of unique technologies of GRS structure developed in Japan, including several new type bridge abutments comprising geosynthetic-reinforced backfill, are reported in this paper.

2. GRS RWS HAVING A STAGED-CONSTRUCTED FULL-HEIGHT RIGID FACING

GRS RWs having a stage-constructed full-height rigid (FHR) facing is now the standard RW construction technology for railways including bullet train lines in Japan, replacing traditional type RWs (Tatsuoka *et al*., 1997, 2007a). Figure 1 shows a typical wall. This new type GRS RW has been constructed at more than 700 sites in Japan, and the total wall length is more than 100 km as of March 2008 (Fig. 2). It is noteworthy that railway engineers in Japan have accepted this new type RW, although railway engineers are generally very conservative in the design of civil engineering structures.

This new type RW has the following features:

(1) The use of a FHR facing that is cast-in-place using staged construction procedures (Fig. 3). The geosynthetic reinforcement layers are firmly connected to the back of the facing, which is essential for high static and dynamic wall stability, as illustrated in Fig. 4.

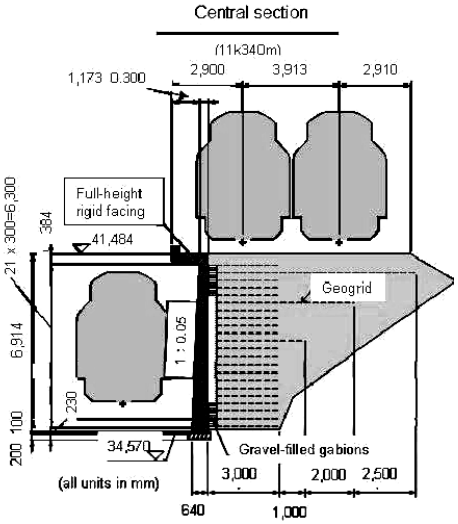

(a) typical cross-section

(b) wall under construction

(c) completed wall

Fig. 1 GRS RW having a FHR facing for one of the busiest rapid transits in Japan (Yamanote Line), near Shinjuku station, Tokyo (constructed during 1995 ~ 2000)

Manuscript received June 4, 2008; revised August 21, 2008; accepted August 21, 2008.

[1] Professor, Tokyo University of Science, Japan (e-mail: tatsuoka@rs.noda.tus.ac.jp).

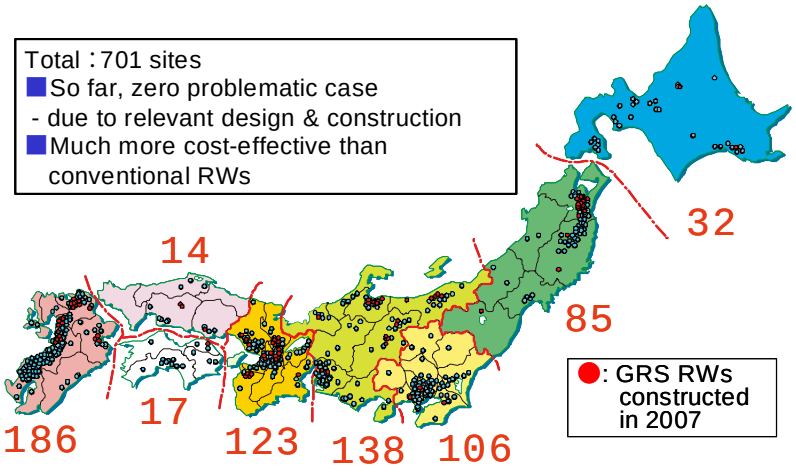

(a)

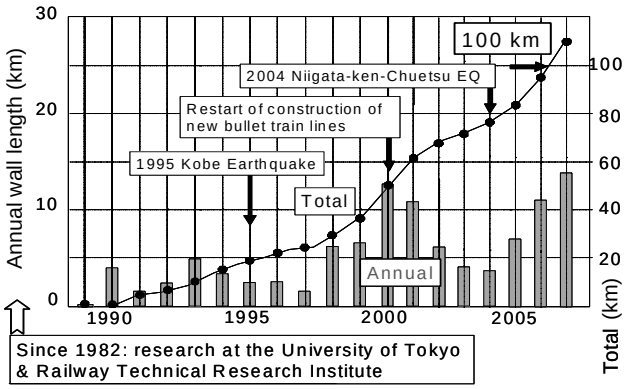

(b)

Fig. 2 (a) Locations; and (b) length of GRS RWs with a staged- constructed FHR facing (as of March 2008)

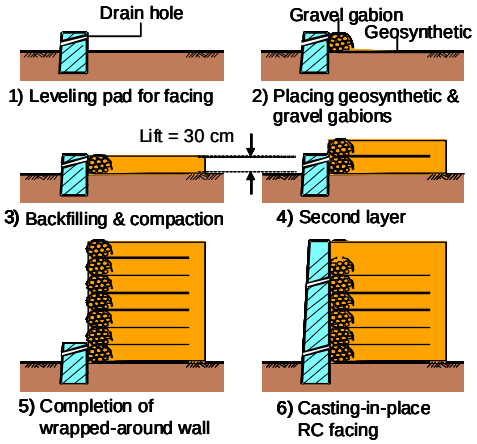

(a) Respective steps

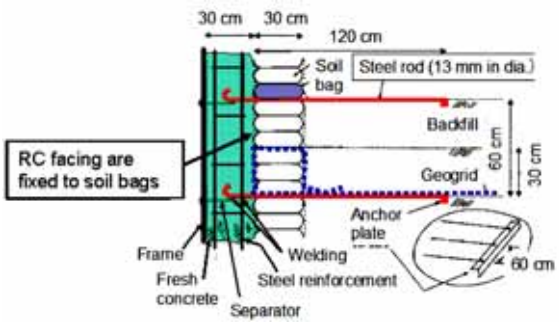

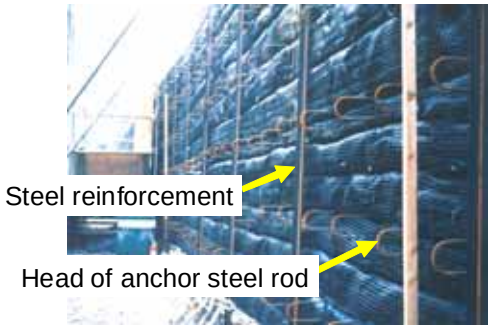

(b) Connection details between the facing and the reinforced backfill (c) Typical wall face before casting-in-place FHR facing

Fig. 3 Staged construction of a GRS RW

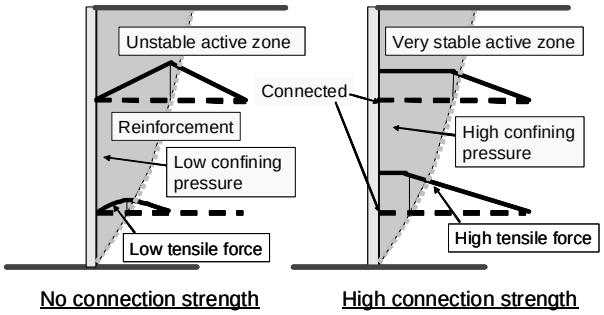

Fig. 4 Effects of firm connection between the reinforcement and the facing (Tatsuoka, 1992)

(2) The use of a polymer geogrid for cohesionless soil to ensure good interlocking and a composite of non-woven and woven geotextiles for high-water content cohesive soils to facilitate both drainage and tensile reinforcing of the backfill. The latter makes possible the use of low-quality on-site soil as the backfill if necessary.
(3) The use of relatively short reinforcement, made possible by using planar geosynthetic reinforcement, which has a relatively short anchorage length necessary to activate the tensile rupture strength.

The staged construction consists of the following steps (Fig. 3(a)): (1) a small foundation element for the facing is constructed; (2) a full-height GRS wall with wrapped-around wall face is constructed by placing gravel-filled bags at the shoulder of each soil layer; and (3) after the major part of ultimate deformation of the backfill and the subsoil layer beneath the wall has taken place, a thin (*i.e.*, 30 cm or more) and lightly steel-reinforced concrete facing is constructed by casting-in-place fresh concrete directly on the wall face, which makes the FHR facing firmly connected to the main body of the backfill. Figure 3(b) shows the details of the connection of the FHR facing to the main body of the reinforced backfill and Fig. 3(c) shows typical view of the wall face before casting-in-place FHR facing at the site presented in Fig. 1. A good connection can be made between the RC facing and the main body of the geosynthetic-reinforced backfill by the following two mechanisms. Firstly, the fresh concrete can be easily penetrated into the inside of gravel-filled gabions through openings of the geogrid. Secondly, extra water from fresh concrete is absorbed by gravel inside the gabions, which prevents negative effects of bleeding phenomenon of concrete. It is to be noted that the gabions wrapped-around with geosynthetic reinforcement and filled with gravel that are placed at the shoulders of soil layers function as; not only (a) a temporary facing structure during construction that makes backfill-compaction more easily and resists against earth pressure generated by compaction and further backfilling at higher levels of the wall; but also (b) a drainage layer after construction; and (c) a buffer that protects the connection between the FHR facing and the reinforcement layers against relative displacement that takes place after construction.

Moreover, concrete form on both sides of the facing and its propping, which becomes more expensive at a high rate as the wall becomes higher, is necessary to construct a conventional RC cantilever RW. On the other hand, only external concrete form without any external propping while not using internal concrete form is necessary with this new GRS RW system (Fig. 3(b)).

With respect to the importance of connecting the reinforcement layers to the rigid facing (Fig. 4), if the wall face is loosely wrapped-around with geosynthetic reinforcement without gabions placed at the shoulder of respective soil layers or the reinforcement layers are not connected to the rigid facing, no tensile force is activated at the wall face in the reinforcement while no significant earth pressure is activated at the wall face. Although a significant reduction in the earth pressure at the wall face has often been claimed as one of the major advantages of GRS RWs, this notion is quite misleading or wrong. This is because no earth pressure at the wall face means no lateral confining pressure activated to the active zone of the backfill, which results in low stiffness and low strength of the active zone and therefore intolerably large deformation and displacement of the active zone (Fig. 4(a)). On the other hand, with this new GRS RW system, as the gabions function as a temporary facing structure, high earth pressure can be activated at the wall face before placing a FHR facing. As wrapping-around geosynthetic reinforcement at the wall face is buried in the fresh concrete layer, eventually the reinforcement layers are firmly connected to the FHR facing and the earth pressure that has been activated to the temporary facing structure comprising gabions wrapped-around with a geogrid is resisted by a FHR facing consisting of a lightly steel-concrete layer and a pile of gabions. The importance of this firm connection for a high wall stability is illustrated in Fig. 4(b). That is, relatively large earth pressure, similar to the active earth pressure that develops in the unreinforced backfill retained by a conventional RW, may be activated on the back of the FHR facing because of a high connection strength between the reinforcement and the facing and a high facing rigidity. This high earth pressure results in high confining pressure in the backfill, therefore high stiffness and high strength of the backfill, which results in significantly better performance of the wall than in the case without using stiff facing or the reinforcement are not firmly connected to a rigid facing (Fig. 4(a)). That is, a substantial reduction of earth pressure is not the target of this new GRS RW technology.

The geosynthetic reinforcement that is required to maintain the stability of GRS RW having a staged constructed FHR facing becomes relatively short when compared to metal strip reinforcement. This is because: (1) the anchorage length of planar geosynthetic reinforcement to resist against the tensile load equal to the tensile rupture strength of reinforcement becomes much shorter; and (2) a FHR facing prevents the occurrence of local failure in the reinforced zone of the backfill by not allowing failure planes to pass through the wall face at an intermediate height. Factor (2) becomes more important when the backfill is subjected to concentrated load on the top of the facing or immediately behind the wall face on the crest of the backfill.

A traditional type RW is basically a cantilever structure that resists against the active earth pressure from the unreinforced backfill by the moment and lateral thrust force at its base (Fig. 5). Therefore, large internal moment and shear force is mobilized in the facing structure while large overturning moment and lateral thrust force develops at the base of the facing. A large stress concentration may develop at and immediately behind the toe on the base of the facing, which makes necessary a pile foundation in usual cases. These disadvantages become more serious at a high rate with an increase in the wall height.

Relatively large earth pressure, similar to the one activated on the traditional type RW, may be activated on the back of the FHR facing of this new type GRS RW because of firm connec-

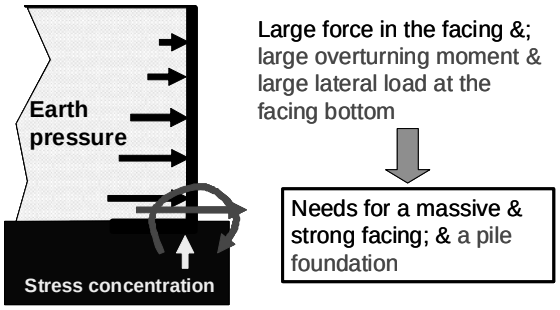

Fig. 5 Traditional type RW as a cantilever structure

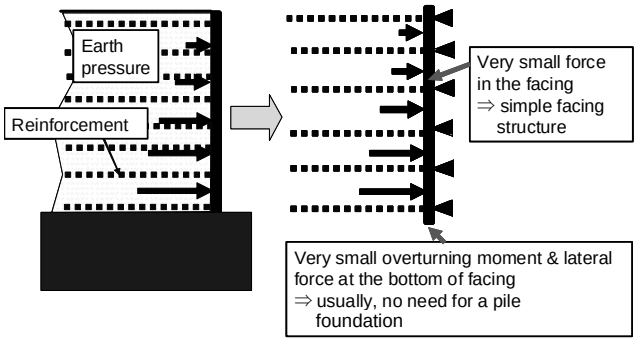

Fig. 6 GRS RW with a FHR facing as a continuous beam supported at many points with a small span (Tatsuoka, 1992; Tatsuoka *et al.*, 1997)

tion between the reinforcement and the FHR facing. Despite the above, as the FHR facing behaves as a continuous beam supported at many levels with a small span, typically 30 cm, only small force is activated in the facing structure (Fig. 6). Because of the above, the facing structure becomes rather simple while the overturning moment and lateral thrust force activated at the facing base becomes small, which makes unnecessary a pile foundation in usual cases. The case histories until today have validated that the GRS RW having a stage-constructed FHR facing is much more cost-effective (*i.e.*, much lower construction cost, much speedy construction using much lighter construction machines), therefore a much less total emission of CO_2 than the traditional type RW. Despite the above, the performance of the new type GRS RW is equivalent to, or even better than, that of traditional type RW.

The elevated transportation structures in Japan have gradually shifted from gentle-sloped embankments towards embankments supported with RWs, recently RC cantilever RWs with a pile foundation, or RC framed structures for higher ones, and then towards GRS RWs having a stage-constructed FHR facing (Fig. 7).

One of the major reasons for a popularity of this new type GRS RW is a high cost-effectiveness when reconstructing gentle slopes of existing embankment to vertical RWs, compared with the traditional method (Fig. 8(a)). In particular, when the stiff bearing soil layer is deep, expensive temporary structures (*i.e.*, ground anchor, sheet piles and concrete form with its propping) becomes necessary with the traditional method. On the other hand, with the new method (Fig. 8(b)), such temporary structures as listed above are not used while the number of construction steps is much smaller, the occupied space is much smaller and the construction period is much shorter. Figures 9 and 10 show

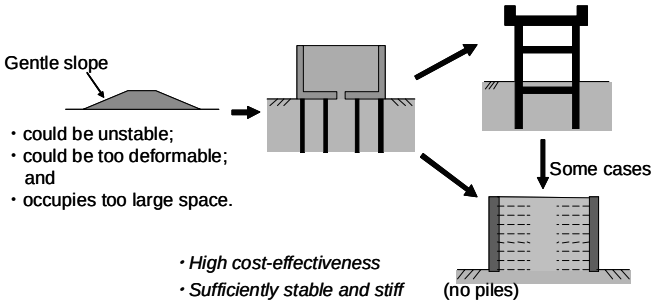

Fig. 7 History of elevated railway and highway structures in Japan

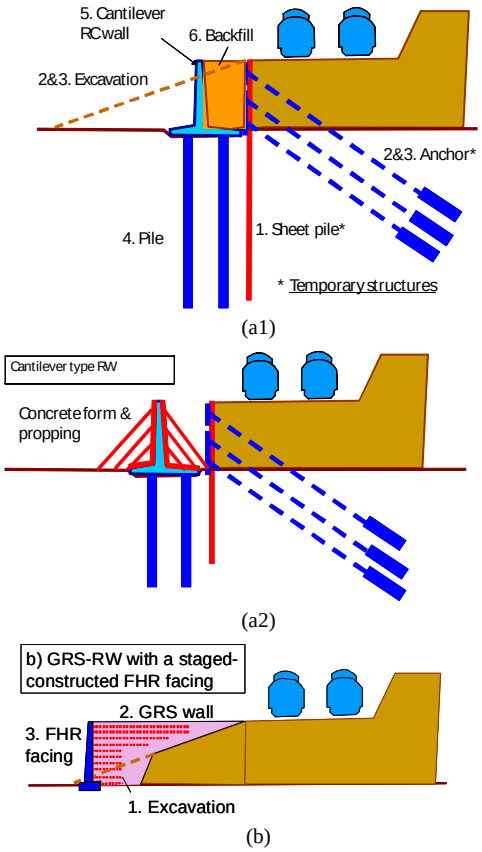

Fig. 8 Reconstruction of a gentle slope of embankment to a vertical wall: (a1) and (a2) the traditional method; and (b) the new method (the numbers indicate construction sequence)

two typical case histories at the early stage showing the above. Moreover, by the new method, taking advantage of a FHR facing supported by reinforcement layers for a full wall height, superstructures that may exert large lateral load, such as electric poles and high noise barrier walls, can be constructed either immediately behind the wall face without a deep pile foundation (Figs. 9(d) and 10(c)), or directly on the FHR facing (Fig. 10(b)). In this respect, three-dimensional effects of FHR facing, as illustrated in Fig. 11(b), make a GRS RW very strong against concentrated load applied to the top of the facing. That is, the FHR rigid facing of this new GRS RW system is continuous not only in the vertical direction but also in the lateral direction. One unit of FHR facing, separated from horizontally adjacent units by vertical construction joints in the facing concrete, has some length,

(a) (b) (c)

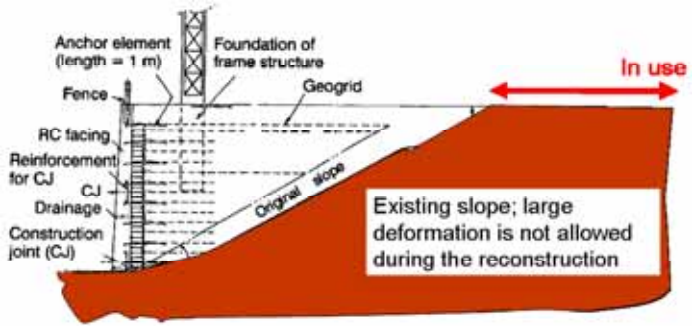

(d)

Fig. 9 (a) Before; (b) during; and (c) after reconstruction of embankment slope to a GRS RW having a FHR facing; and (d) typical cross-section, a yard for bullet trains (Shinkan-Sen) in Nagoya; average wall height = 5 m; total length = 930 m; and construction period = 1990 ~ 1991 (Tatsuoka *et al.*, 1997)

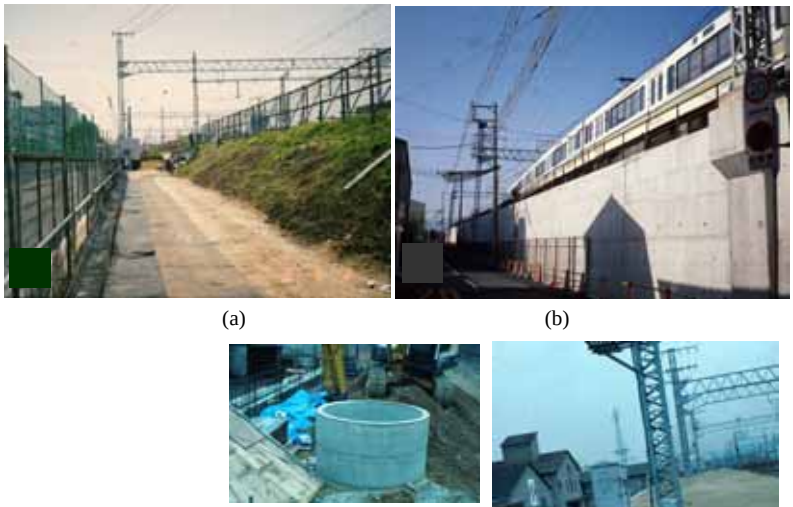

(a) (b)

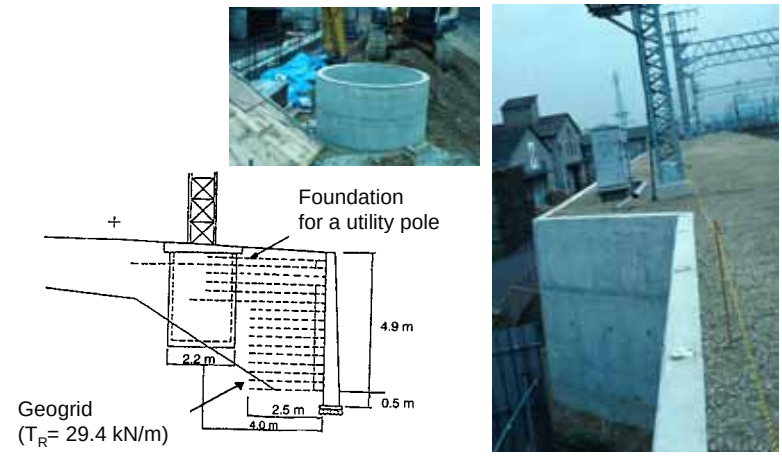

(c)

Fig. 10 (a) During; and (b) after reconstruction of embankment slope to GRS RWs having a FHR facing; and (c) a foundation for a utility pole constructed inside the geogrid- reinforced backfill; a rapid transit between Osaka and Kobe; average wall height = 5 m; total length = 1,300 m; and construction period = 1991 ~ 1992 (Tatsuoka *et al.*, 1997)

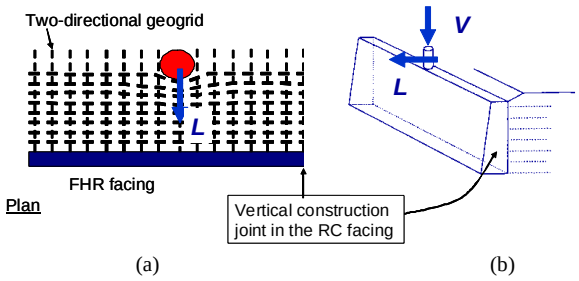

Fig. 11 3-D resistance of FHR facing/geogrid system against lateral load acting to; (a) a vertically long structure located inside the reinforced zone; and (b) the top of the facing (Tatsuoka *et al*., 1997)

usually 20 m. Therefore, the whole FHR facing unit can resist against concentrated vertical or lateral load applied to the facing top with a help of all the reinforcement layers that are connected to the facing unit. Moreover, a foundation that is embedded inside the reinforced backfill can exhibit large lateral resistance against the lateral load acting in the direction normal to the wall face (Fig. 11(a)). Figure 10(c) shows a case history showing the above. Tamura *et al*. (1994) and Tateyama *et al*. (1994a) reported full- scale loading tests performed to validate the advantages described above. On the other hand, when a discrete panel facing is used, some costly measures become necessary to resist against concentrated load (in particular lateral load) that is activated directly to or immediately behind the facing on the crest of the backfill (Fig. 12).

The features of FHR rigid facing described above become most advantageous when a FHR facing functions as a foundation for a super-structure. The most typical application is bridge abutments made of GRS RWs having a staged constructed FHR facing. Figure 13 shows one of many bridge abutments of this type that have been constructed until today. At this site, three abutments were constructed for railways (Seibu Line) in Tokyo. During peak commuting times, passenger trains ran the bridge every three minutes at a high speed. The bridge abutments of GRS RWs were constructed directly on a Kanto Loam soil deposit without using a pile foundation. Any problems by significant settlement of the bridge girder due to the train load did not take place. The use of a FHR facing made the design and construction of these GRS bridge abutments feasible, as a GRS-RW with a FHR facing can effectively resist the seismic lateral loads of a bridge girder. This feature was confirmed by performing full-scale loading tests at the site (Tatsuoka *et al*., 1997).

No case of collapse and excessive deformation has been reported among many case histories of this new type GRS RW (Fig. 2). This may be attributed mainly to the following factors: (a) a good compaction of the backfill is ensured due to a relative small vertical spacing of geogrid layers (*i.e.*, 30 cm) and no rigid facing is existing during backfill compaction; (b) all potential problems due to deformation and displacements of wall and ground can be recognised and dealt with before the construction of a FHR facing; (c) gabion bags stacked immediately behind the FHR facing ensure good drainage and act as a buffer when relative displacement tends to take place between the facing and the reinforced backfill after having been opened to service; (d) a planar geogrid is used, rather than metal strips (which are much easier to pull out); and (e) the GRS RWs are designed against high seismic loads; it was confirmed that duly designed and constructed GRS

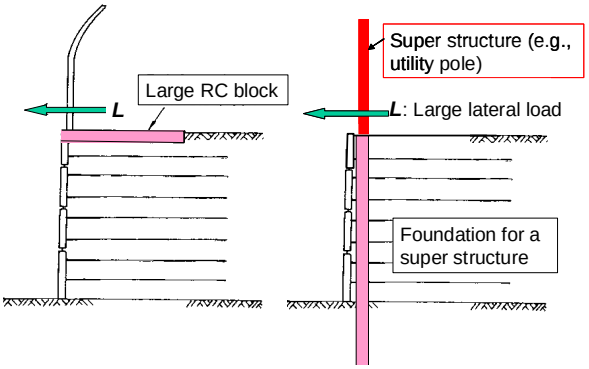

Fig. 12 Measures required to resist against lateral load activated immediately behind a discrete panel facing (Tatsuoka *et al*., 1997)

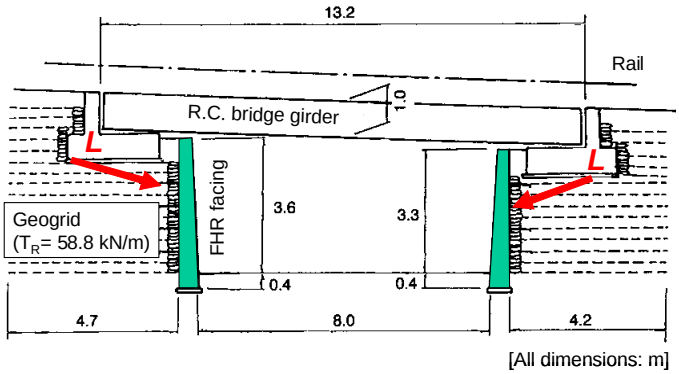

Fig. 13 Bridge abutments of GRS RWs having a staged constructed FHR facing, near Sakuradai Station, Seibu Ikebukuro Line, Tokyo (Tatsuoka *et al*., 1997); (a) elevation of the bridge and adjacent GR RW; (b) view of the completed bridge; and (c) lateral loading test of a bridge abutment (Tatsuoka *et al*., 1997)

RWs can survive such severe earthquakes as the 1995 Kobe Earthquake (Tatsuoka *et al*., 1998). The design rupture strength of geogrid is usually determined by the aseismic design, and, therefore, the design rupture strength is not reduced to account for creep rupture by long-term static loads. Yet, no case history in which the wall has exhibited noticeable creep deformation has been reported. Tatsuoka *et al*. (2004, 2006) and Tatsuoka (2008) proposed a new method by which the rupture strength of geosynthetic reinforcement to be used in both aseismic and static designs is not reduced for creep rupture.

3. RECONSTRUCTION OF COLLAPSED EMBANKMENTS AND RWS

Numerous embankments and traditional type RWs collapsed by floodings and earthquakes in the past in Japan (*e.g.*, Fig. 14). Previously, most of the collapsed soil structures were reconstructed to respective original traditional types despite that they are not cost-effective and their resistance against flooding and seismic loads is sufficient.

From the beginning of the 1990's, reconstruction of railway embankments that collapsed by heavy rainfalls and floodings to embankments having geosynthetic-reinforced steep slopes or GRS RWs having a stage-constructed FHR facing or their com-

Fig. 14 Gravity type RW without a pile foundation at Ishiya-gawa that collapsed during the 1995 Kobe Earthquake (Tatsuoka *et al*., 1997, 1998)

bination started based on the successful experiences described above. Figure 15 shows a typical case of the above. This reconstruction method was employed also in many other similar cases after this case (Tatsuoka *et al*., 1997).

High performance during the 1995 Kobe Earthquake of a GRS RW of this type that had been constructed at Tanata validated its high-seismic stability (Fig. 16). Many gentle slopes of embankment and traditional type RWs that collapsed during the 1995 Kobe Earthquake and subsequent earthquakes were reconstructed to GRS RWs having a stage-constructed FHR facing (Tatsuoka *et al*., 1977, 1998). Figure 17 shows reconstruction of one of the three railway embankments supported by gravity type RWs at the slope toe that totally collapsed during the 2004 Niigata-ken Chuetsu Earthquake. GRS RWs having a FHR facing were constructed at these three sites because of not only much lower construction cost and much higher stability (in particular for soil structures on a steep slope), but also much faster construction and a significant reduction of earthwork when compared to reconstruction to the original embankments. The new type GRS RWs are also much more cost-effective and the construction is faster than bridge type structures. During this earthquake, road embankments collapsed at numerous places in mountain areas and many of them were reconstructed to GRS RWs or embankments having geosynthetic-reinforced steep slopes.

The March 25th 2007 Noto-hanto Earthquake caused severe damage to embankments of Noto Toll Road (opened in 1978). The north part of this road runs through a mountainous area for a length of 27 km. The damage concentrated into this part, where eleven high embankments filling valleys were extensively collapsed (Koseki *et al*., 2008). The collapsed embankments were basically reconstructed to GRS RWs while ensuring the drainage of ground and surface water.

(a)

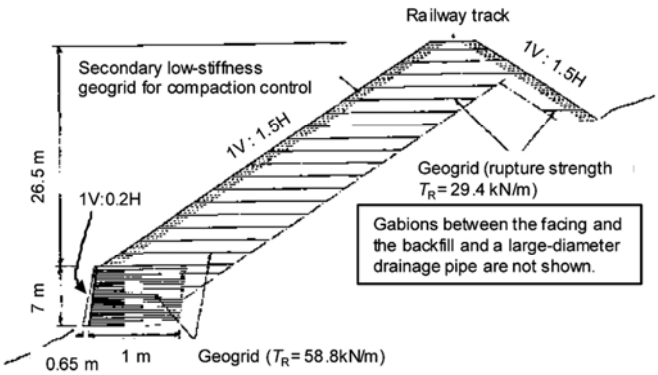

(b)

(c)

Fig. 15 (a) Railway embankment damaged by rainfall in 1989; (b) reconstructed cross-section; and (c) after reconstruction in 1991 (Tatsuoka *et al*., 1997; 2007)

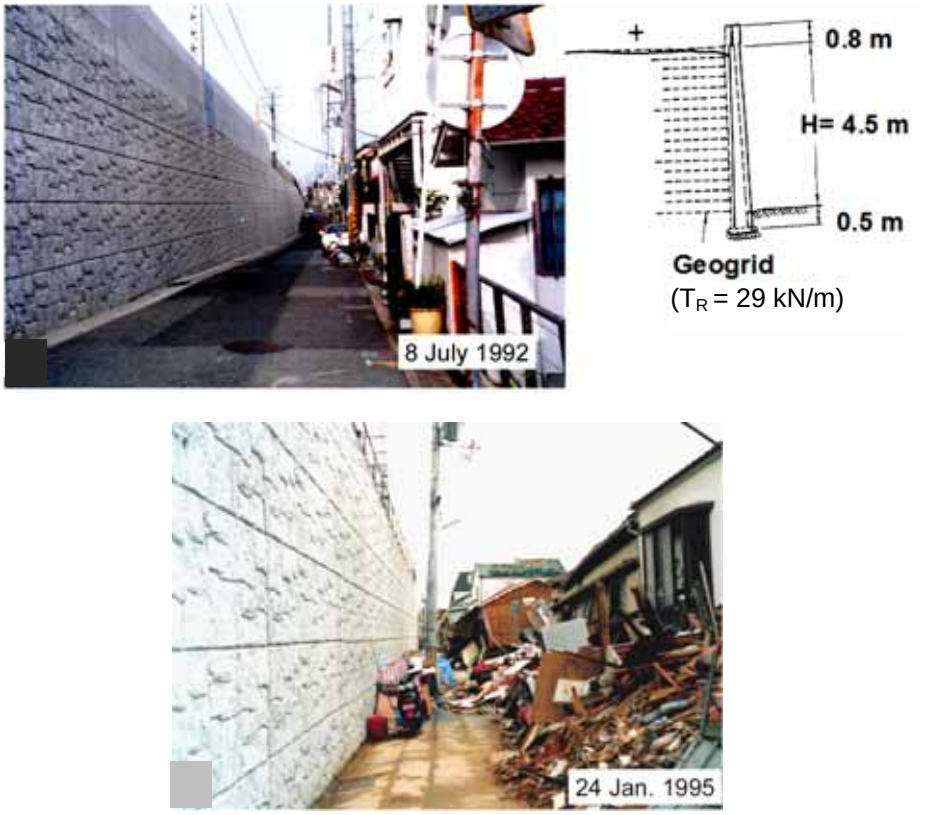

Fig. 16 GRS RW having a FHR facing at Tanata; (a) immediately after construction and a typical cross-section; and (b) one week after the 1995 Kobe Earthquake (Tatsuoka *et al*., 1997, 1998)

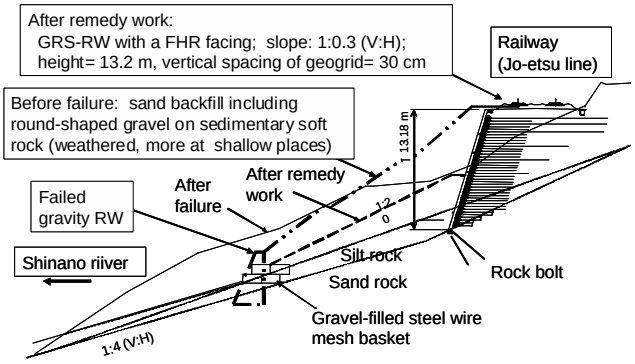

(a)

(b) (c)

Fig. 17 (a) Railway embankment that collapsed during the 2004 Niigata-ken Chuetsu Earthquake and its reconstruction to a GRW RW having a FHR facing; (b) the wall during reconstruction; and (c) the completed wall (Morishima *et al*., 2005)

After many successful case histories, as described above, the geosynthetic-reinforcing technology is now widely accepted to reconstruct embankments and traditional RWs that collapsed by floodings and earthquakes. This technology was also used to rehabilitate an old earth-fill dam having a crest length of 587 m and a height of 33.6 m in the north of Tokyo (Fig. 18). When constructed about 80 years ago, this was the largest earth-fill dam in Japan. The reservoir is exclusively for water supply in Tokyo, which will become extremely important at the time of disasters, including seismic ones, because of its ability of sending raw water in gravity flow to several water treatment plants downstream. A 17 m-high counter-weight fill was constructed on the downstream slope of the dam aiming at a substantial increase in the seismic stability of the dam to prevent vast disaster to a heavily populated residential area that had developed in front of the dam recent years. Due to a severe space restriction, the counter-weight fill was made steep by reinforcing using HDPE geogrids over a total area of 28,500 m^2 in the fill.

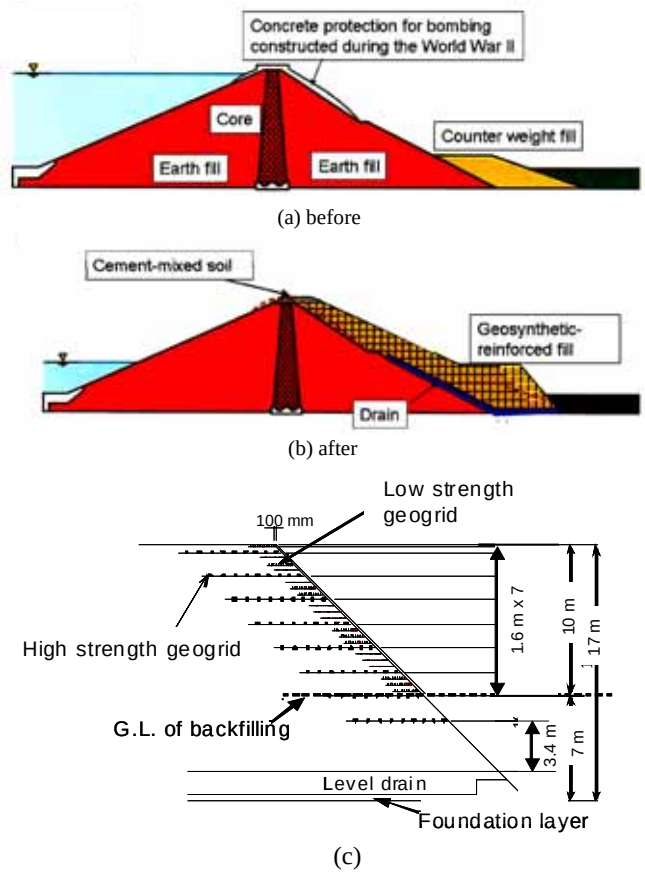

Fig. 18 Shimo-Murayama dam in Tokyo: (a) before; and (b) after rehabilitation; and (c) geogrid-reinforced counter-weight fill (Maruyama *et al.*, 2006)

4. HIGH GEOGRID-REINFORCED SOIL WALLS

At the Fujisan-Shizuoka Airport in Japan, which is now under construction, two high GRS walls (21.1 m and 16.7 m-high) were constructed to preserve the natural environment, which consists of steep swamp areas in front of the walls (Fig. 19(a)). These areas should have been buried if gentle-sloped embankments had been constructed as planned originally. Figures 19(a) and 19(b) show the front view and cross-section of one of the two walls. As the walls support the airport runway, minimum residual displacements at their crest are required. A sufficiently high seismic stability is another important design issue. The backfill was well-graded gravelly soil, which was compacted very well to an average degree of compaction higher than 95% of the maximum dry density obtained using compaction energy 4.5 times higher than the standard Proctor (Fig. 19(d); Tatsuoka, 2008).

The monitoring of the walls (Fig. 19(e)) showed very small deformation during construction and nearly zero residual deformations after wall completion, indicating a very high stability of the walls. This case history indicates that long-term residual deformation of GRS structures can be restrained very effectively by highly compacting the backfill despite the use of so-called extensible reinforcement (*i.e.,* geogrid). More details of the project are described in Tatsuoka (2008). The analysis of tensile load in the geogrid is described below.

The recorded time histories of geogrid tensile strain also exhibited nearly no increase after wall completion, as typically seen from Fig. 20(a). Analysis of these data based on an elasto-viscoplastic model of the geogrid developed based on laboratory test data showed that the tensile load in the geogrid tends to noticeably decrease with time after wall completion, therefore, creep rupture failure of the geogrid by the end of the design life is unlikely (Fig. 20(b)). In this analysis, the drop in the tensile load (T) after one year until 50 years is very small, as the tensile strain (ε) according to the extrapolated ε – time relation exhibits very small change during this period and the viscous response has become very weak after a large drop in T. The reduction of the tensile force in the geogrid with time, when it takes place as in this case, is due to not only the viscous properties of the geogrid but also compressive creep strains in the horizontal direction of the backfill caused by the tensile force in the reinforcement. This case history indicates that the assumption in current practice that the tensile force mobilised in the geosynthetic reinforcement in a GRS structure is kept constant over-estimates the possibility of creep rupture failure of geosynthetic reinforcement. It must be particularly the case when GRS structures are adequately designed and constructed against high seismic loads.

5. BRIDGE ABUTMENTS CONSISTING OF GEOSYNTHETIC-REINFORCED BACKFILL

A traditional type bridge comprises a single simple-supported girder supported by a pair of abutments via fixed (or hinged) and moveable shoes (or bearings), or multiple simple-supported girders supported by a pair of abutments and a single or multiple pier(s) via shoes. The traditional type abutment, which may be a gravity structure (unreinforced concrete or masonry) or a RC structure, has the following many drawbacks (Fig. 21). Firstly, as the abutment is a cantilever structure that retains unreinforced backfill (Fig. 5), earth pressure activated on its back induces large internal force as well as large thrust force and overturning moment at the bottom of the abutment. Therefore, usually, the abutment becomes massive, while a pile foundation becomes necessary unless the supporting ground is strong enough. This drawback becomes more serious at an increasing rate with an increase in the wall height. Secondly, although only small movement is allowed once constructed, the backfill are constructed after the abutments are constructed.

(a)

(b)

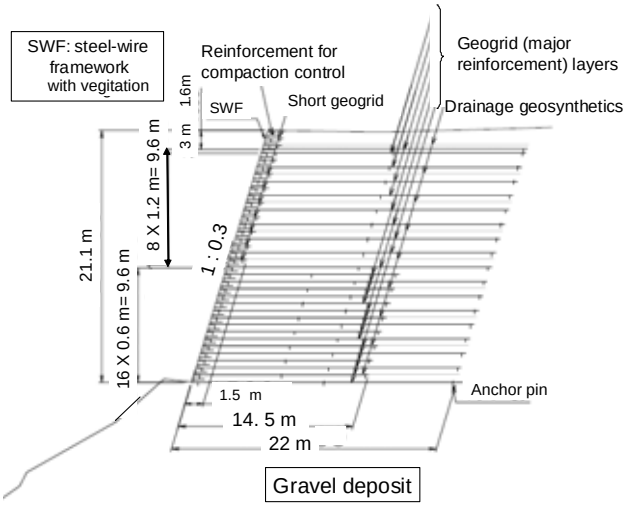

(c)

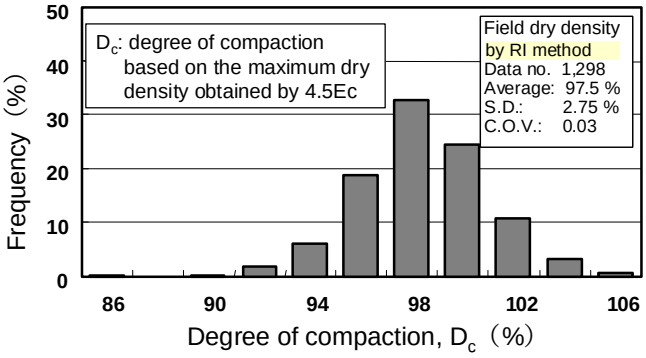

(d)

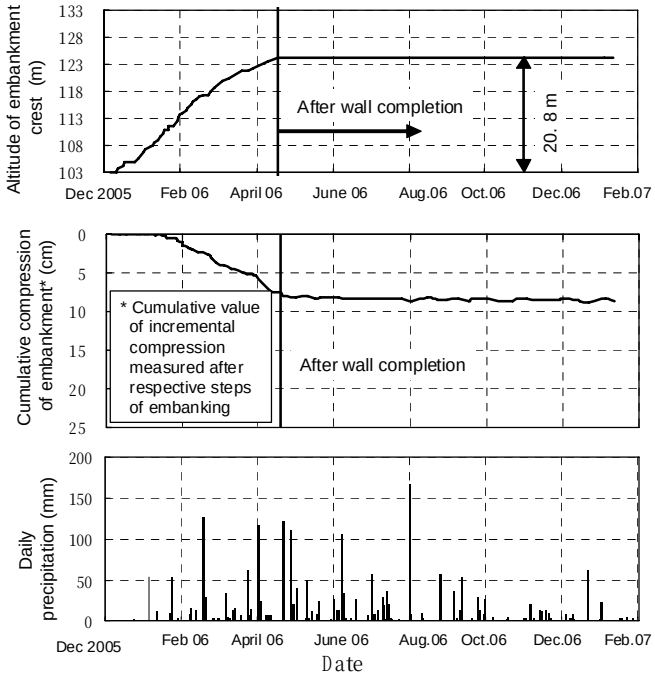

(e)

Fig. 19 High GRS walls for Fujisan-Shizuoka Airport; (a) wall in valley 1, 2nd Nov. 2007; (b) wall in valley 2; (c) cross-section of wall in valley 2; and (d) degrees of compaction of the backfill, wall in valley 2; (e) monitored behaviour of wall in valley 2 (Fujita *et al.*, 2008; Tatsuoka, 2008)

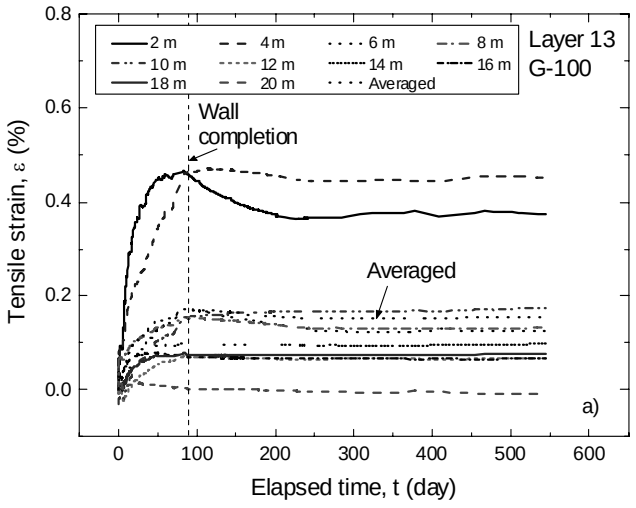

(a)

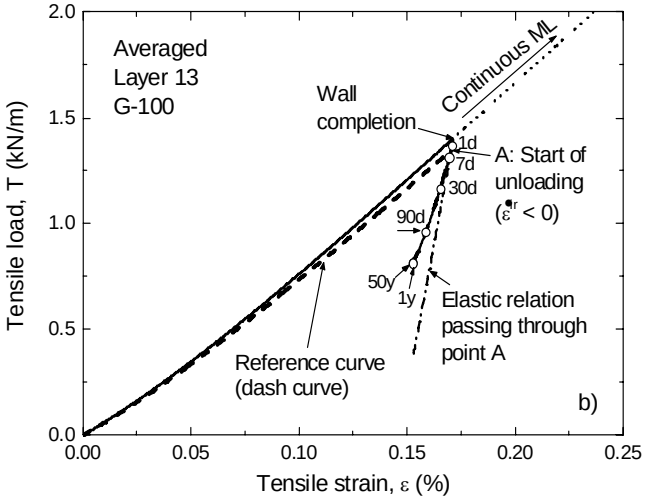

(b)

Fig. 20 (a) Time histories of individual and average tensile strains; and (b) tensile load-average strain relations predicted for 50-year service, geogrid layer 13 (G-100) in wall in valley 2 (Kongkitkul *et al*., 2008; Tatsuoka, 2008)

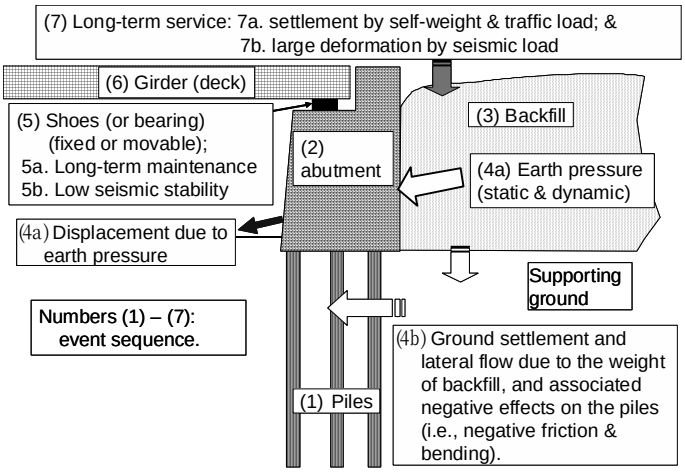

Fig. 21 Traditional type bridge abutments

Hence, when constructed on soft ground, many piles may become necessary to prevent movements of the abutments due to earth pressure as well as settlement and lateral flow in the subsoil caused by the backfill weight. Large negative friction may develop along the piles. The piles may become much longer than the wall height when the soft ground is thick. Thirdly, the construction and long-term maintenance of girder shoes (*i.e.*, girder bearings) and connections between simple-supported girders are generally costly. Moreover, the shoes and connections are weak points when subjected to seismic loads. Fourthly, a bump may be formed behind the abutment by long-term settlement of the backfill due to its self weight and traffic loads. Lastly, the seismic stability of the backfill is relatively low; the backfill may deform largely by seismic loads. Furtheremore, the abutment supporting the girder via a fixed shoe is also relatively low, while the girder may dislodge at a movable shoe.

To alleviate these problems with the conventional bridge type, three new bridge types have been proposed (Fig. 22). The integral bridge (Fig. 23) has been proposed to alleviate problems with the structural part (usually reinforced concrete) of the traditional type bridge. This type is now widely used in the UK, the USA and Canada, mainly due to low construction and maintenance cost resulting from no use of shoes and the use of a continuous girder. Furthermore, the seismic stability of integrated bridge is higher than the traditional type (as shown later). However, as the backfill is not reinforced, thus not unified to the structural part, the backfill and the structural part do not help each other. Therefore, this new bridge type cannot alleviate some old problems with the traditional type bridges (Fig. 23(a)) and their static and seismic stability is not very high. Moreover, as the girder is integrated to the abutments, seasonal thermal expansion and contraction of the girder results into cyclic lateral displacements of the abutments (Fig. 23(b)). This results in; (1) development of high earth pressure on the back of the abutment (*i.e.*, facing); and (2) large settlements in the backfill (England *et al*., 2000; Hirakawa *et al*., 2006, 2007a). The effects of daily thermal effects are negligible.

Figure 24 shows several geotechnical measures to improve the performance of the backfill behind the abutment (Tatsuoka, 2004; Tatsuoka *et al*., 2005). To increase the seismic stability of the backfill, the Japanese railway engineers constructed a trapezoidal zone of well-compacted well-graded gravelly soil (type a1 in Fig. 24). However, the performance of this type during several earthquakes in Japan was generally poor. Watanabe *et al*. (2002) and Tatsuoka *et al*. (2005) confirmed the above by performing model shaking table tests. They also showed that the seismic stability of a similar type consisting of a trapezoidal zone of cement-mixed gravel (type a2, Fig. 24) is not sufficiently high.

Taking advantages of the stage-construction procedure (Fig. 3), many bridges comprising a pair of GRS RWs with a FHR facing that support a simple-supported girder (type b1 in Fig. 24) were constructed (Tatsuoka *et al*., 1997). Figure 13 shows a typical case history. Although this bridge type, called the GRS- RW bridge (Fig. 25), is more cost-effective than the traditional type (Fig. 21), it has the following problems: (1) The length of the girder is limited due to low stiffness of the backfill supporting the sill beam. (2) The construction and long-term maintenance of shoes is costly. Moreover, the shoes are weak against seismic loads. These problems are common with all bridge types presented in Fig. 24. (3) Although the seismic stability of GRS RWs with a FHR facing is very high

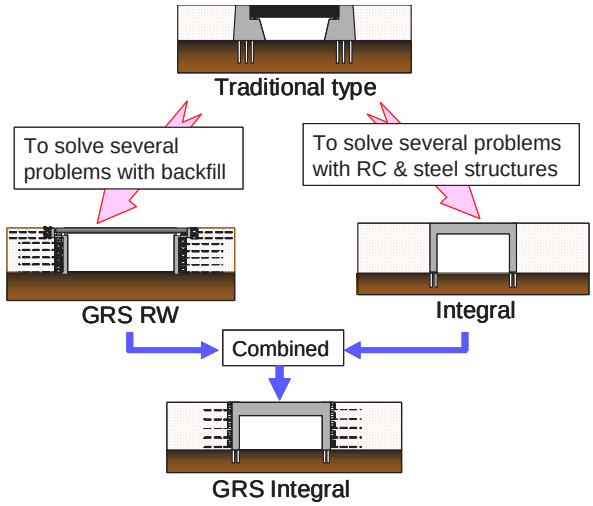

Fig. 22 Development of new type bridges

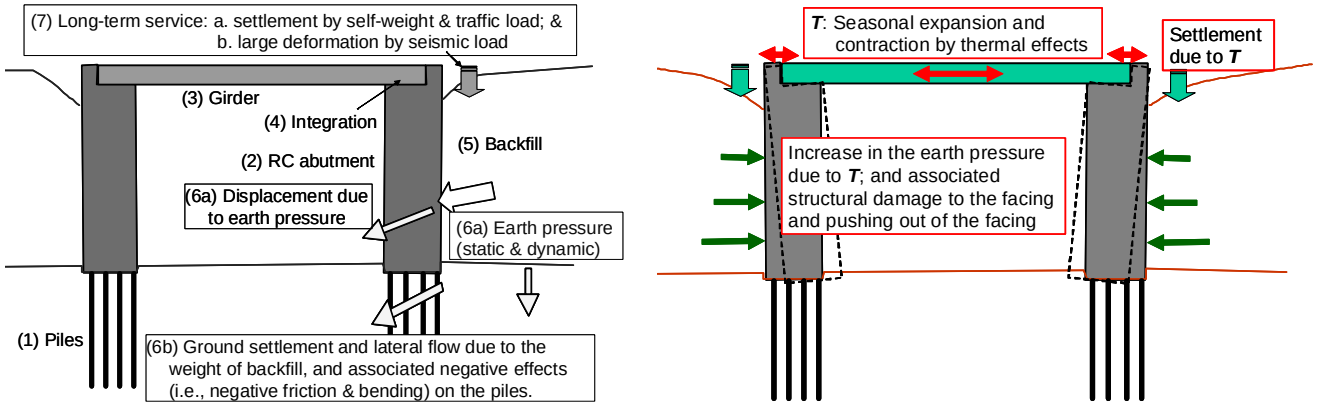

Fig. 23 Integral bridge: (a) construction sequence and associated problems; and (b) a new problem

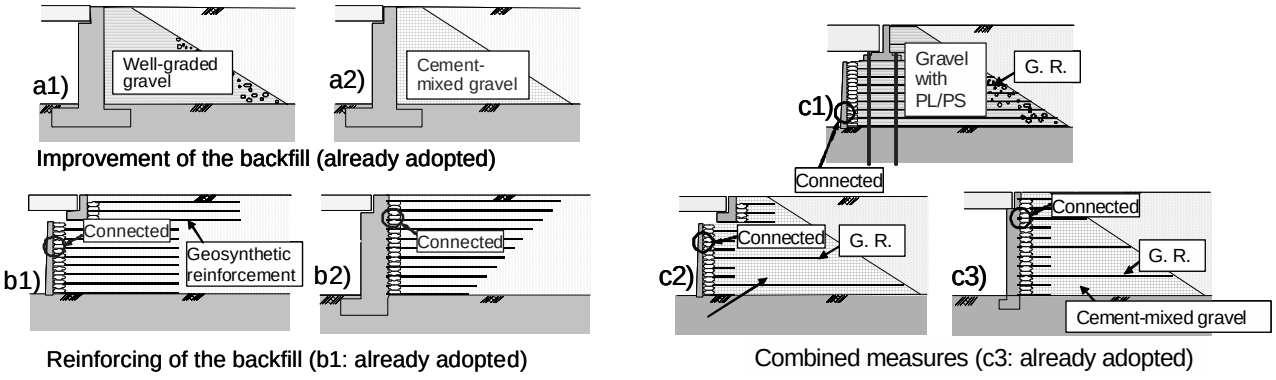

Fig. 24 Different proposals to improve the performance of the backfill (Tatsuoka *et al.*, 2005)

(*e.g.*, Tatsuoka *et al.*, 1998; Koseki *et al.*, 2006), it is not the case with the sill beam supporting the girder via a fixed shoe, because the mass of the sill beam is much smaller than the girder while the anchorage capacity of the reinforcement layers connected to its back is small due to their shallow depths. Type b2 (Fig. 24), placing a girder on the top of the FHR facing via a shoe, exhibits no residual displacements of the girder and is dynamically more stable than type b1 (Watanabe *et al.*, 2002; Tatsuoka *et al.*, 2005). However, problem 2) is still unsolved.

To alleviate these problems (1) and (2) with type b1 (*i.e.*, GRS-RW bridge, Fig. 25), it is very effective to vertically preload the reinforced backfill and then maintain relevant vertical prestress, typically about a half of the preload, in the backfill during long-term service (*i.e.*, the preload (PL) and prestress (PS) technology; type c1 in Fig. 24). The difference between the prestress and the prestress should be larger than the design load. The effectiveness of this technology was found by laboratory model tests (Shinoda *et al.*, 2003(a)) and then validated by good

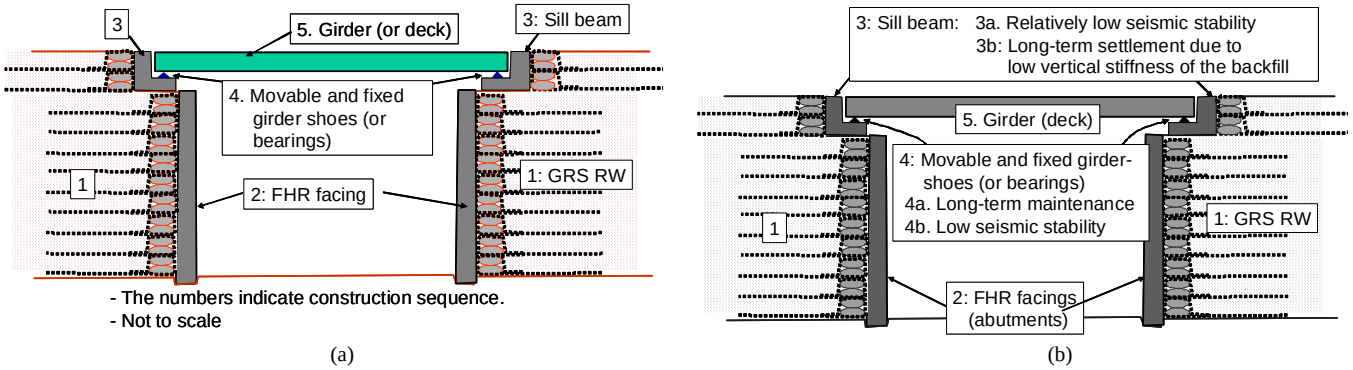

Fig. 25 GRS-RW bridge: (a) construction sequence; and (b) unsolved old problems

long-term performance of a prototype railway bridge pier (Uchimura *et al*., 2003a, 2005). Moreover, Nakarai *et al*. (2002), Uchimura *et al*. (2003b) and Shinoda *et al*. (2003b) showed that the seismic stability of PL-PS reinforced soil structure is very high if high prestress can be maintained during seismic loading by using a ratchet mechanism to fix the ends of the tie rods used to apply prestress. However, any prototype bridge abutment of type c1 using a ratchet connection mechanism has not been constructed, because possible long-term maintenance works of the ratchet system are not preferred by practicing engineers.

Abutment types c2 and c3 (Fig. 24) were then proposed, which combine, respectively, types b1 and b2 with type a2. Type c3 was adopted by Japanese railway engineers and the first prototype was constructed for a new bullet train line in Kyushu (Fig. 26). The abutment was constructed by the staged construction procedure placing a girder on the top of the RC facing via a fixed shoe (Fig. 27). The traditional RC abutment (Fig. 21) laterally supports the unreinforced backfill, which may activate large static and dynamic earth pressure on the back of the facing. In contrast, with abutment type c3, the reinforced backfill laterally supports a thin RC facing that supports the girder, without the backfill activating static and dynamic earth pressure on the facing. Following this project, a number of similar bridge abutments were constructed recently and are being planned. Despite the above, type c3 abutments are not free from several problems due to the use of girder shoes.

To alleviate these many problems with the traditional type bridge (Fig. 21) as well as those with the integral bridge (Fig. 23) and new types described in Fig. 24 (including the GRS-RW bridge, Fig. 25), Tatsuoka *et al.* (2007b, 2008a, b and c) proposed another new type bridge, called the GRS integral bridge (Fig. 28). This new type bridge combines the integral bridge and the GRS- RW bridge taking advantages of their superior features while alleviating their drawbacks. The GRS integral bridge is actually the same as a bridge consisting of type c3 abutments (Fig. 26) from which shoes are removed while integrating the girder to the abutments. With the GRS integral bridge, it is not necessary to cement-mix the backfill in usual cases. If it is necessary to ensure very high performance of the bridge, particularly during severe earthquakes, the backfill may be cement-mixed as abutment type c3.

The GRS integral bridge (Fig. 28) has the following features in structure and construction:

(1) The backfill is reinforced with geosynthetic reinforcement layers that are firmly connected to the back of the FHR facings (*i.e.*, the abutments).

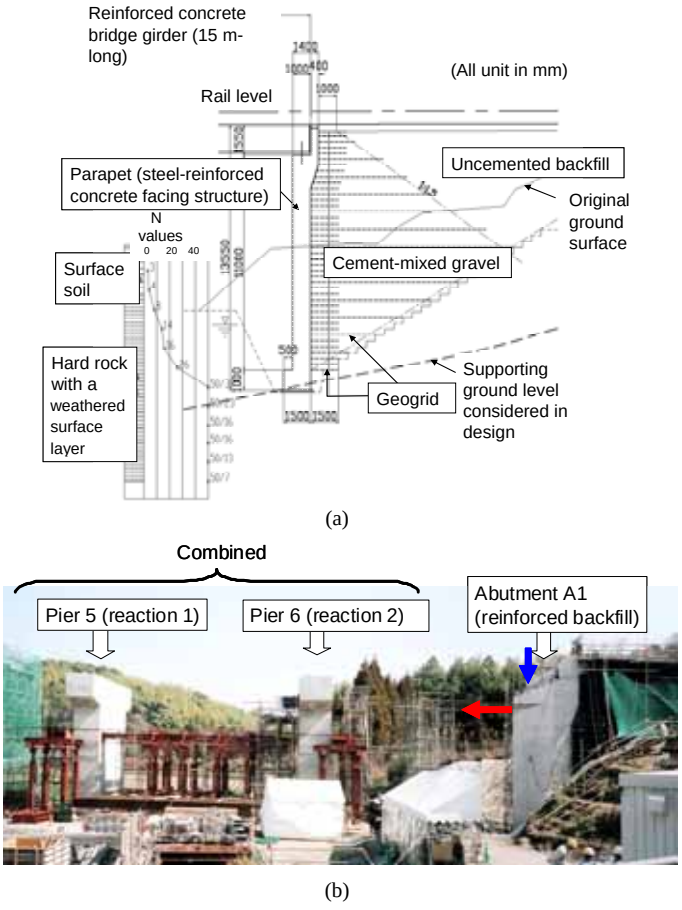

Fig. 26 A prototype bridge abutment of type c3 (Fig. 24) at Takada, Kyushu, for a new bullet train line (Tatsuoka *et al.*, 2005); (a) structural details; and (b) lateral and vertical loading tests of the facing

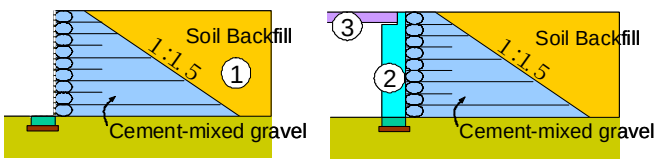

Fig. 27 Staged construction (type c3 in Fig. 24)

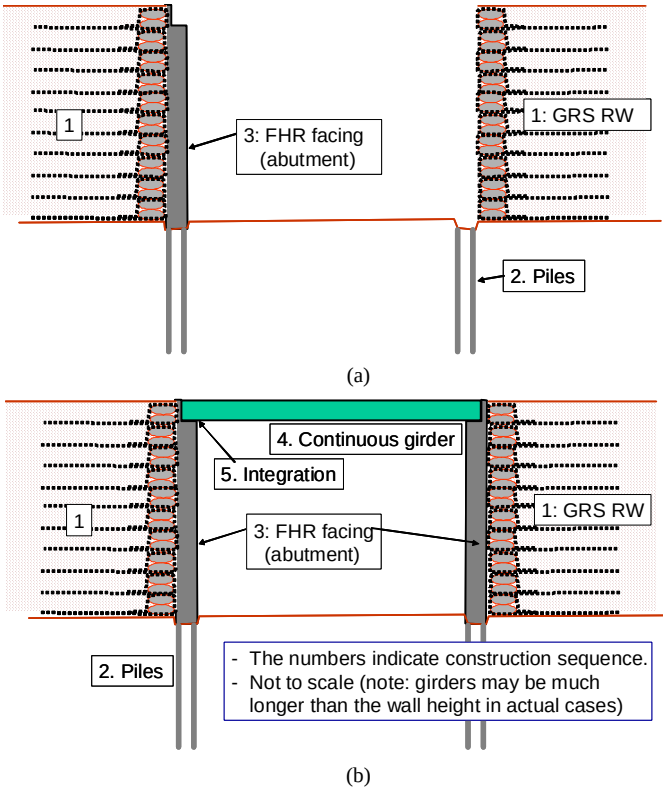

Fig. 28 GRS integral bridge

(2) The abutments are constructed by the following staged construction procedure:

(a) A pair of GRS walls (without a FHR facing, the wall face being wrapped-around with geogrid reinforcement) are first constructed.

(b) Pile foundations to support the FHR facings are constructed, if necessary. If the deformation of the supporting ground by the construction of the backfill is not significant, pile foundations may be constructed before the GRS walls for better constructability.

(c) FHR facings are constructed by casting-in-place fresh concrete on the wall face.

(d) A continuous girder is placed on and integrated to the crest of the facings.

This staged construction procedure is a modification of the one described in Fig. 3 and, therefore, it has the same advantages. That is, firstly the connection between the reinforcement and the facing is not damaged by differential settlement between the facing and the backfill during wall construction. Then, construction of abutments on relatively compressible subsoil without using heavy piles becomes possible. Secondly, by compacting well the backfill allowing sufficient outward movements at the wall face, sufficient tensile force can be mobilized in the reinforcement during the construction of GRS walls (w/o a FHR facing).

With traditional type bridges (Fig. 21) and GRS-RW bridges (Fig. 25), the length of a single simple-supported girder is restricted to avoid excessive lateral seismic load to be activated to the abutment on which a fixed shoe supports the girder. With integral bridges (Fig. 23), the girder length is limited to avoid excessive large cyclic lateral displacements at the top of the abutments by seasonal thermal expansion and contraction of the girder. The girder length is restricted also to limit the lateral seismic load activated to the abutments. With the GRS integral bridge, such restrictions as above are much looser, therefore, the actual length of the girder relative to the abutment height could be generally much longer than the one depicted in Fig. 28. The girder length limit for GRS integral bridges would be larger than the value for conventional type integral bridges, which is presently specified to be 50 ~ 60 m in the USA to restrict the maximum thermal deformation of the girder to four inches (about 10 cm). More research will be necessary in this respect.

Figure 29 compares the characteristic features of the four different bridge types described in the precedent sections. The rating presented in this figure is only an approximation. That is, the full point allocated to each item is three, which is reduced one by one when any of the listed negative factors *A* to *G* is relevant. The horizontal accelerations at which the respective bridge models collapsed in the shaking table tests explained below are listed. A total full point equal to nine is given only to the GRS integral bridge.

Bridge type	Cost & period of construction	Maintenance cost	Seismic stability	Total
Traditional	1 *A, B*	1 *C, D*	1 *F, G* 252 gal*	3
Integral	2 *B*	1 *D, E*	2 *F* 641 gal*	5
GRS RW	3	1 *C, D'*	2 *G'* 589 gal*	6
GRS Integral	3	3	3 1,048 gal*	9

(* Failure acceleration in model shaking table tests)

A = needs for massive abutments because of cantilever structure.

B = needs for piles because of; (1) cantilever-structure abutments; and (2) limited allowable post-construction displacements despite the construction of backfill after piles & abutments.

C = high cost for construction and long-term maintenance of girder shoes (*i.e.*, bearings) and their low seismic stability.

D = long-term backfill settlement by self-weight and traffic loads.

D′ = long-term settlement of sill beam.

E = lateral cyclic displacements of the abutment caused by thermal expansion and contraction of the girder, resulting in high earth pressure and large backfill settlement by the dual ratchet mechanism.

F = large backfill settlement and large dynamic earth pressure

G = low seismic stability due to independent performance of two abutments

G′ = low seismic stability of the sill beam.

Fig. 29 Rating of four different bridge types based on cost and performance (the higher points, the higher rating)

6. MODEL TESTS

Static cyclic loading tests: A series of static tests were performed on model under plane strain conditions (Fig. 30(a)) to evaluate the effects of cyclic lateral displacements of the facing on the performance of the backfill (Aizawa *et al*., 2007; Hirakawa *et al*., 2007b). The backfill was air-dried poorly graded sub-angular sand, Toyoura sand (D_r = 90%). Figure 30(c) shows the test cases performed in the present study. Two conditions at the facing bottom (**H** and **F**) were employed. The wall height, *H*, is equal to 50.5 cm for the hinge support (**H**) and 48 cm for the free condition (**F**). At a distance of 11.5 cm down from the facing top, the FHR facing was cyclically displaced at a displacement rate of 0.004 mm/sec (converted to the value at the facing top). Two cyclic displacement modes **A** and **AP**, which simulate the behaviours of the integral bridges that are completed in summer and fall respectively, were employed (Fig. 30(c)).

Figure 31 is a typical test result when the backfill is unreinforced; the facing bottom is hinged; and the ratio of amplitude of displacement at the facing top *D* to the wall height *H* (= 50.5 cm) = 0.6% in the active displacement mode. This figure shows the time histories of; b) the lateral displacement at the facing top, *d*; c) the backfill settlement, S_g, at different distances *L* from the back of the facing; and d) the total earth pressure coefficient, $K = 2Q/(H^2\gamma)$, where, *Q* is the total earth pressure per width of the facing measured with nine local two-component load cells (measuring normal and shear loads) arranged on the back of the model FHR facing (Fig. 30(a)); and γ is the dry unit weight of the backfill (1.60 gf/cm^3). It may be seen that, even by small lateral displacements of the facing, the peak earth pressure in the respective cycles increases significantly with cyclic loading. After five cycles (*i.e.*, after five years with the prototype), the *K* value becomes higher than three. Correspondingly, the backfill settles down significantly more at places closer to the facing. At L/H = 5 cm/50.5 cm ≈ 0.1, the settlement, S_g, after five cycles exceeds 1% of the wall height, *H*. These trends are due to the dual ratchet mechanism in the backfill (England *et al*., 1995, Tatsuoka *et al*., 2008a, b, c), which is explained later in this paper. With full- scale integral bridges, by this earth pressure increase, the facing structure may be structurally damaged while the facing bottom may be strongly pushed out, developing a large bump behind the facing.

Figure 32 summarizes the peak values of *K* in each cycle, K_{peak}, at selected numbers of loading cycle, *N*, plotted against *D/H* when the backfill is either unreinforced or reinforced (without and with reinforcement connected to the facing). In these tests, the facing displacement is active only and the facing bottom is hinge-supported. The trend that the earth pressure at a given cycle increases with *D/H* may be seen, which is consistent with the previous studies by Ng *et al*. (1998) and England *et al*. (2000). The mode test result presented in Fig. 32(a) is also consistent with the full-scale field behaviour for three years (*i.e.*, *N* = 3) plotted in the same figure (Hirakawa *et al*., 2006). The increasing rate of K_{peak} with *D/H* is strong when the backfill is unreinforced (Fig. 32(a)). It may also be seen that the increase in K_{peak} with cyclic loading is largest when the backfill is reinforced but without connection of the reinforcement to the facing (Fig. 32(b)). In this case, because of no connection of reinforcement to the facing, despite the backfill is reinforced, significant active failure takes place with large settlements in the backfill immediately behind the facing, similarly as the unreinforced backfill. Yet, the lateral stiffness of the reinforced backfill is higher than the unreinforced backfill because of a smaller active zone due to reinforcing effects. Therefore, the force necessary to push back the facing from an active state becomes larger. Highly increased earth pressure may structurally damage the facing and/or may push out the bottom of the facing in the prototype. On the other hand, when the reinforcement is connected to the facing, an increase in the earth pressure with cyclic loading is smallest (Fig. 32(c)). Even in this case, the increase in the earth pressure is not small. However, as the facing is anchored by many reinforcement layers, this increase does not damage the facing and does not push out the facing bottom by the mechanism illustrated in Fig. 6.

Figure 33(a) shows the relationship between the backfill settlement at the neutral state (*i.e.*, $d = 0$) at 5 cm back of the facing and the number of loading cycles, *N*, when D/H = 0.2%. The facing displacement is either only active or equally active and passive while the facing bottom is hinge-supported. The backfill is either unreinforced or reinforced (with and without the connection of reinforcement to the facing). Figure 33(b) compares the backfill settlement when D/H = 0.2% and 0.6% while the facing displacement is only active. The following trends may be seen from Figs. 33(a) and (b):

(1) The backfill settlement increases with *D/H*.

(2) The settlement for the same *D/H* is larger when the facing displacement is only active than when equally active and passive, because an active wedge can be formed more easily in the former case.

(3) The settlement is largest when the backfill is unreinforced, whereas it is nearly zero when the backfill is reinforced with the reinforcement connected to the facing. This is because, when the reinforcement is connected to the facing, the confining pressure in the backfill is maintained high, which makes the backfill less deformable, and membrane effects of the reinforcement prevent the formation of an active wedge.

(4) When the backfill is reinforced but the reinforcement is not connected to the facing, the settlement is not small, which may not be allowable if it takes place in the prototype.

As shown below, when the reinforcement is not connected to the facing, the settlement immediately behind the facing becomes considerably larger when the facing bottom is free than when the facing bottom is hinge-supported. On the other hand, when the reinforcement is connected to the facing, the backfill settlement when the facing bottom is free is very small as when the facing bottom is hinge-supported.

High passive earth pressures and large settlements in the backfill associated with the formation of an active wedge by cyclic lateral displacement of facing with small amplitude described above are due to the dual ratchet mechanism in the backfill, as explained below. Figure 34 shows the time histories of lateral displacement at the facing top and the backfill settlement (L = 5 cm) presented in Fig. 31 that are interpreted by this mechanism, explained in Fig. 35. That is,

(1) Suppose that a small active displacement of the facing takes place and small active sliding develops forming an active wedge (*i.e.*, process S → A1 in Figs. 34 and 35).

(2) Subsequently, the facing is subjected to small passive displacement (*i.e.*, process A1 → P1). In this process, the active

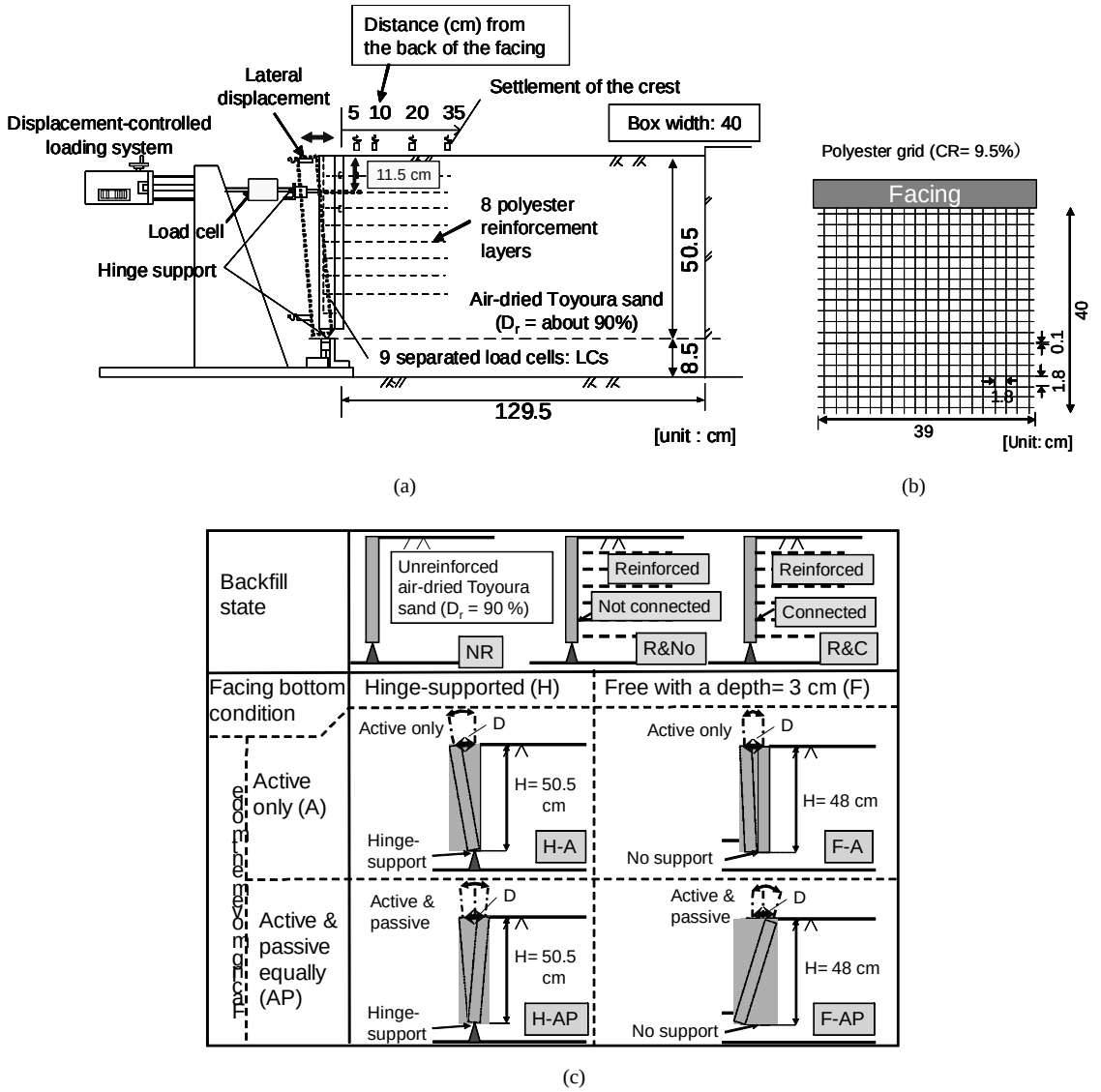

Fig. 30 Static lateral cyclic loading tests of the facing; (a) sand box (conditions R&C and H-A); (b) model reinforcement; and (c) loading test cases (Aizawa *et al*., 2007; Hirakawa *et al*., 2007b)

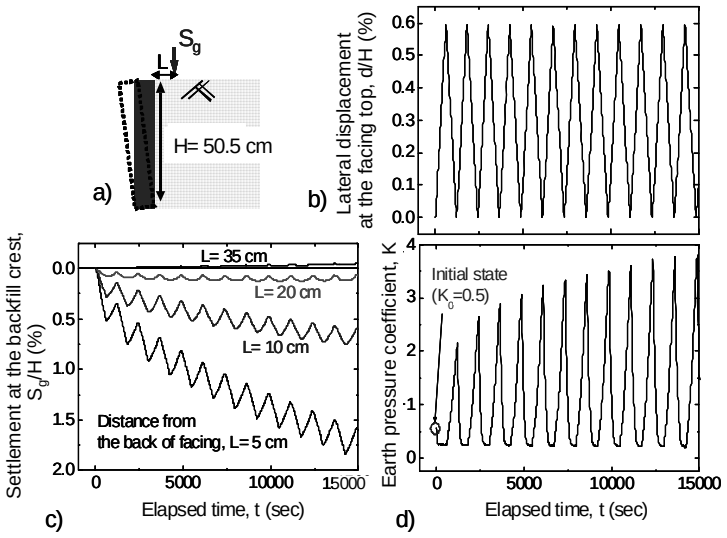

Fig. 31 (a) Test method; and time histories of (b) horizontal movement at the facing top, (c) backfill settlement; and (d) total earth pressure, unreinforced Toyoura sand (case NR **and** H-A**, Fig. 30c) (Aizawa *et al*., 2007; Hirakawa *et al*., 2007b)**

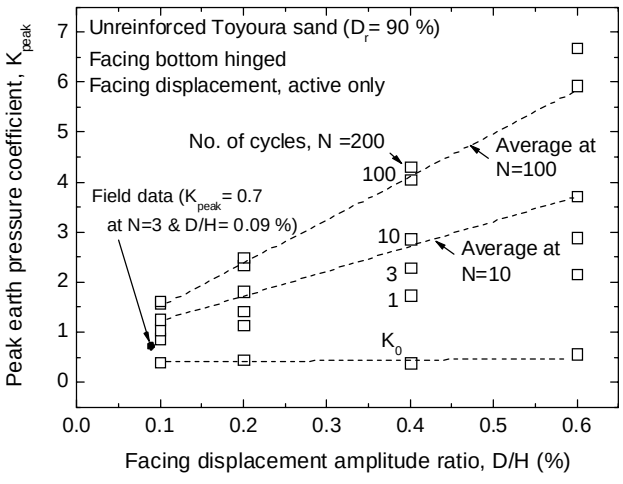

(a)

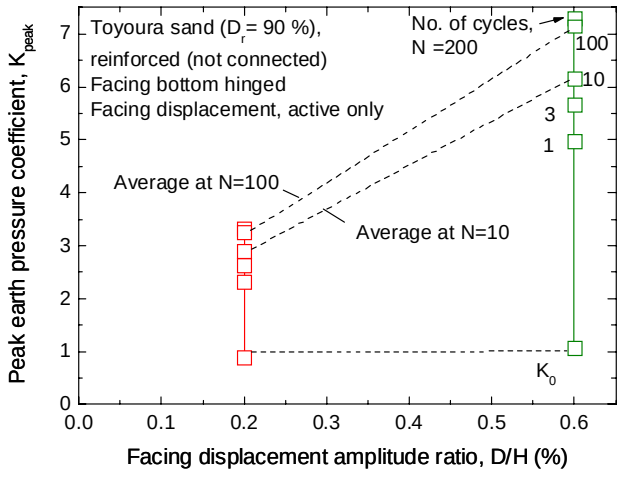

(b)

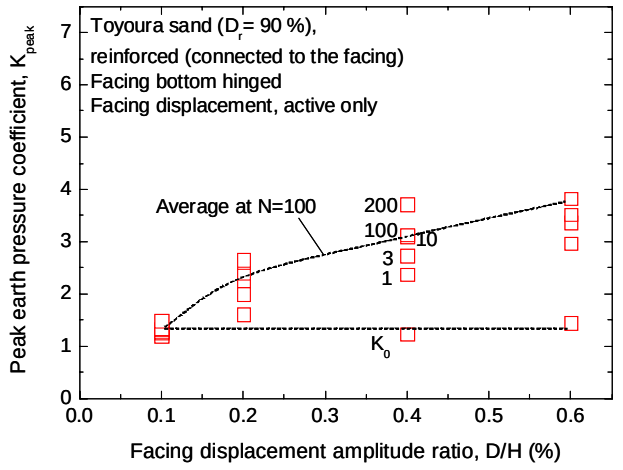

(c)

Fig. 32 Peak earth pressure coefficients, K_{peak}, versus facing displacement, D/H (case H-A); (a) unreinforced backfill: and reinforced backfill; (b) without and; (c) with reinforcement connected to the facing

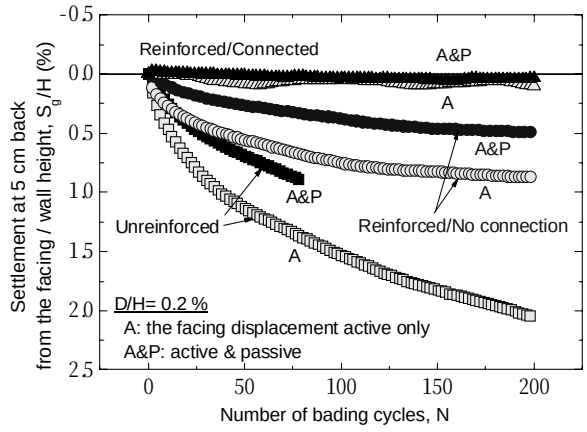

(a)

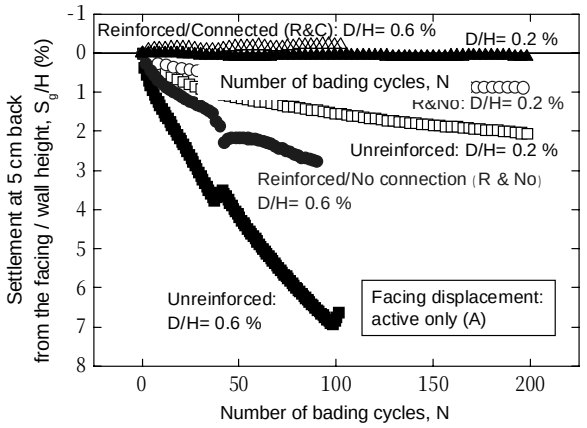

(b)

Fig. 33 Backfill settlement (when d = 0) at 5 cm back of the facing in unreinforced and reinforced backfill with the facing bottom hinge-supported; (a) D/H = 0.2% (cases A and P): and (b) D/H = 0.2% and 0.6% (case A)

sliding is not re-activated, because the passive deformation of the passive wedge zone, which is much larger than the active wedge, is easier to take place. The active wedge deforms in the passive mode as part of the passive zone.

(3) When the second small active displacement of the facing takes place, the active sliding further develops (*i.e.*, process P1 → A2), while the part outside the active wedge in the passive zone does not deform.

(4) When the facing is subjected to the second small passive displacement (*i.e.*, process A2 → P2), again, the active sliding is not re-activated, while the passive deformation further develops.

These processes (1) to (4) are repeated in the course of cyclic lateral displacement of the facing. Although it is small in each cycle, the active sliding accumulates with cyclic loading as illustrated in Fig. 34(a) (*i.e.*, the active ratchet mechanism). The accumulated active sliding soon reaches the value at which the active failure takes place during monotonic active loading, as shown in Fig. 36. Although it is also small in each cycle, the passive strain in the passive zone accumulates with cyclic loading (Fig. 34(a)), which gradually increases the passive earth pressure with cyclic loading (*i.e.*, the passive ratchet mechanism). As the passive displacement of the facing when the passive failure takes

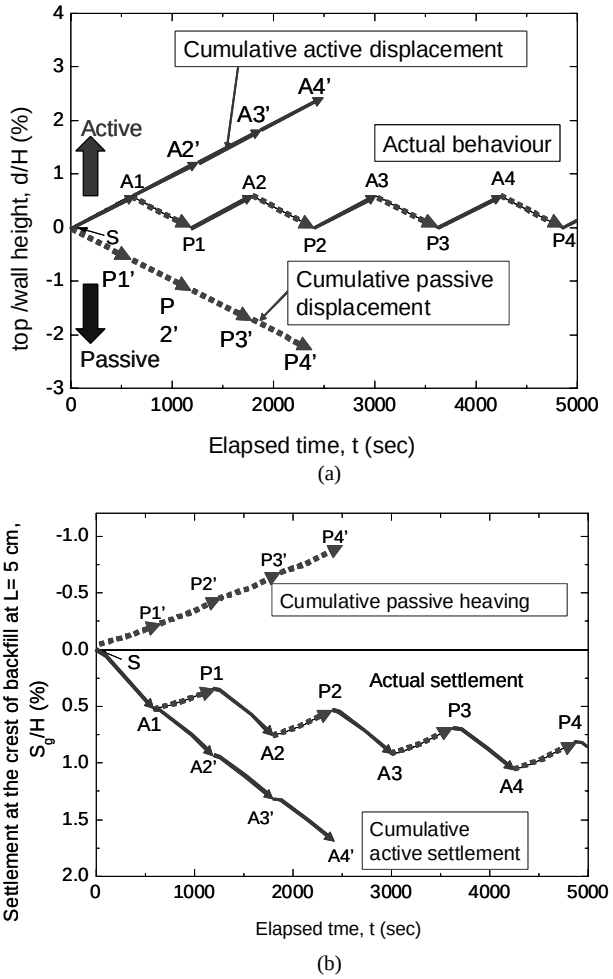

Fig. 34 Interpretation by the dual ratchet mechanism of: (a) lateral displacement at the facing top; and (b) backfill settlement

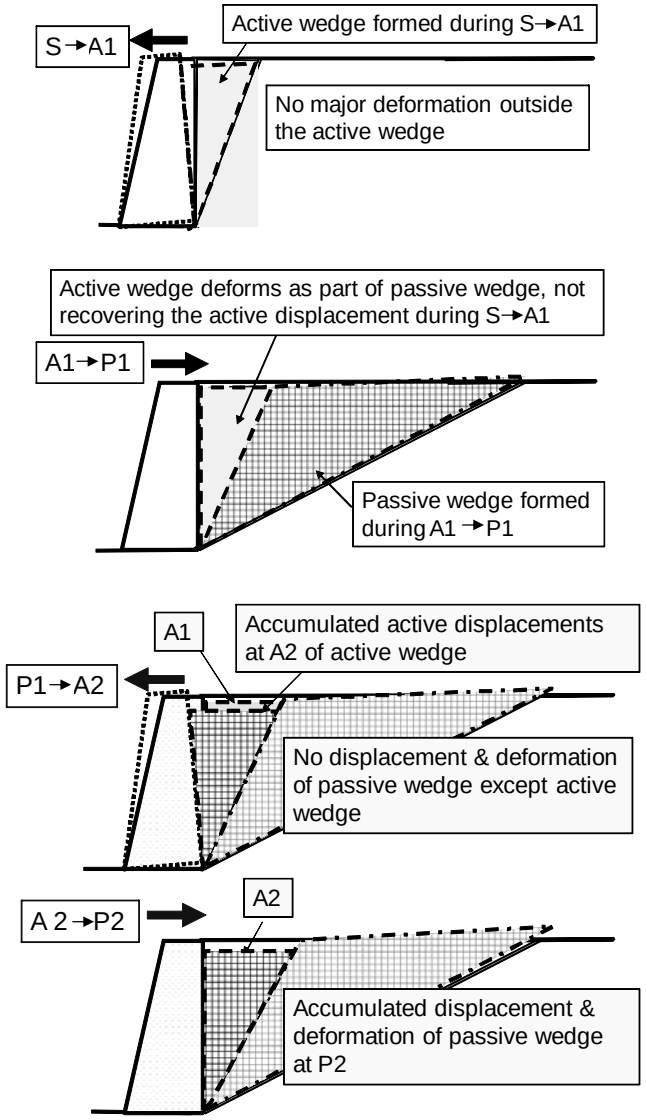

Fig. 35 Dual ratchet mechanism when the facing bottom is hinge-supported

place during monotonic passive loading is very large (Fig. 36), the active failure takes place far before the passive failure takes place during cyclic loading. At the crest of the backfill, large settlement takes place associated with accumulation of active sliding with cyclic loading as seen from Fig. 34(b). At the same time, heaving takes place outside the active zone in the passive zone by cumulative passive deformation of the passive zone, as illustrated in Fig. 34(b). The actual settlement that takes place in the backfill is a summation of those due to the dual ratchet mechanism explained above and those by compressive volumetric strains accumulated in the backfill due to negative dilatancy caused by cyclic shear straining.

The dual ratchet mechanism explained above is similar in nature to the cyclic strain-hardening effect that was observed in cyclic plane strain compression/extension tests on Toyoura sand (Masuda *et al*., 1999). Tatsuoka *et al*. (2003) explained the cyclic strain-hardening effect by a proportional rule for hysteresis loops as well as a drag rule for skeleton curves. They showed that, by this effect, the peak-to-peak secant modulus of hysteresis stress-strain loop for a fixed strain amplitude increases with cyclic loading. By this effect, the peak earth pressure in the respective cycles increases with cyclic loading in the model tests performed in the present tests. An increase in the minimum earth pressure with cyclic loading can be explained by another mechanism, as

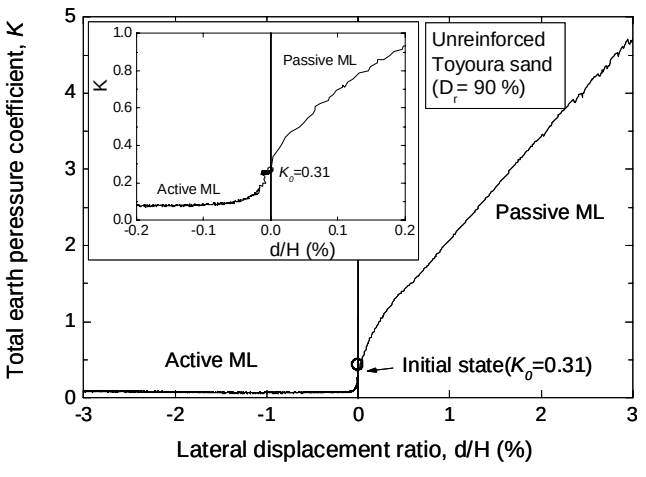

Fig. 36 Earth pressure during active and passive monotonic loadings on unreinforced backfill, the facing bottom hinged

well as cyclic strain-hardening effect. That is, in active monotonic loading, the active earth pressure increases with an increase in the active displacement of the facing after it has exhibited the minimum value (*i.e.*, the active earth pressure when the peak angle of friction is mobilised). This is due to a decrease in the friction angle caused by post-peak strain-softening in the shear band (*i.e.*, the active failure plane). Although it is subtle, this trend may be seen in the relation from an active monotonic loading test presented in Fig. 36. More research will be necessary to accurately simulate the dual ratchet phenomenon observed in the model tests.

It is to be noted that the dual ratchet mechanism becomes active also when relative lateral displacements take place repeatedly between the facing and the backfill, without the residual displacement developing only toward the active direction of the facing, during a seismic event. It is the case with integral bridges subjected to seismic loadings, where the relative distance between a pair of abutment does not change during seismic loading. In that case, large backfill settlement may take place in the backfill while the earth pressure on the back of the facing may increase largely. This is another drawback of the integral bridge. It is shown later that these drawbacks with integral bridges can be effectively alleviated by reinforcing the backfill with geosynthetic reinforcement layers that are connected to the back of the facing.

When the facing bottom is not supported by a pile foundation therefore rather free for lateral sliding and rotation, the facing bottom can be easily pushed out, therefore the active failure takes place more easily in the unreinforced backfill (Fig. 37(a)) and the settlement significantly increases (Figs. 37(b) and 38), associated with a significant decrease in the earth pressure (Fig. 38). This model test result shows that detrimental effects of lateral cyclic loading at the facing caused by seasonal thermal compression and expansion of the girder become more serious when the facing bottom is not supported firmly by a pile foundation or another equivalent firm foundation.

In summary, an abutment comprising a FHR facing and backfill becomes very stable against lateral cyclic displacements caused by seasonal thermal expansion and contraction of the girder when the backfill is reinforced with reinforcement layers that are connected to the facing (*i.e.*, the GRS integral bridge, Fig. 28). When the reinforcement is not connected to the facing, this high performance cannot be expected.

Shaking table tests: To validate high dynamic stability of the GRS integral bridge, shaking table tests were performed on models of the four bridge types described in Fig. 22 (Aizawa *et al.*, 2007; Hirakawa *et al.*, 2007b; Tatsuoka *et al.*, 2007b; 2008a, b and c; Fig. 39). The supporting ground and backfill were made of air-dried Toyoura sand having $D_r \approx 90\%$. On the crest of the backfill, a surcharge of 1 kPa made of lead shots was placed to simulate the weight of road base for railways or highways. A length similitude ratio equal to 1/10 was assumed. The abutments (*i.e.*, facings) of the four models were made of duralumin, all having a height of 51 cm and a bottom width equal to 20 cm. The back and bottom faces of the abutments were made rough by gluing sand paper (#150). A mass of 205 kg was attached to the center of a 61 cm-long model girder to make the equivalent length equal to 2 m (*i.e.*, 20 m in the assumed prototype scale). No pile foundation supporting the abutment was used to examine the most critical failure mode of these bridge types.

(a)

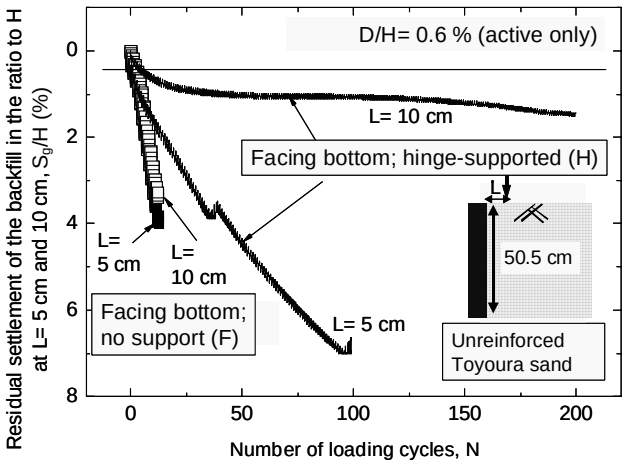

(b)

Fig. 37 Effects of footing bottom condition on the behaviour of unreinforced backfill, D/H = 0.6% and active only; (a) failure mode; and (b) backfill settlement

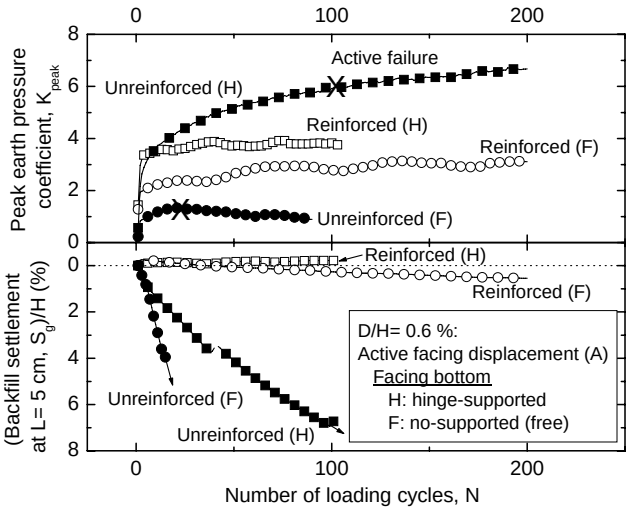

Fig. 38 Effects of backfill-reinforcing and facing bottom conditions

The reinforcement was a grid made of phosphor bronze consisting of 17 longitudinal strands with high rupture strength, 359 N per strand (Fig. 40). The covering ratio was 10.1%. The surface of the strands was made rough by gluing sand particles, with a friction angle equal to 35 degrees at confining pressure equal to 50 kPa. The respective reinforcement layers were fixed to the back of a 59 cm-wide facing by using six bolts. With the models of integral bridge and GRS integral bridge, the girder and facings were connected to each other by using an L-shaped steel fixture

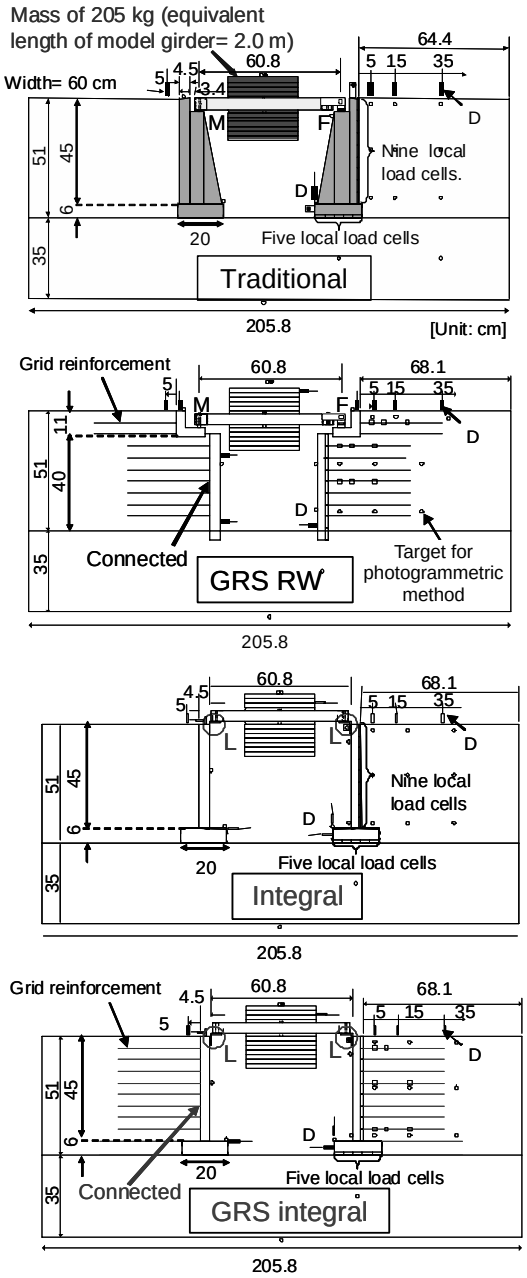

Fig. 39 Models for shaking table tests, air-dried Toyoura sand (D_r = 90%); D: displacement transducer; M: movable (sliding) shoe; F: fixed (hinged) shoe; and L: L-shaped metal fixture

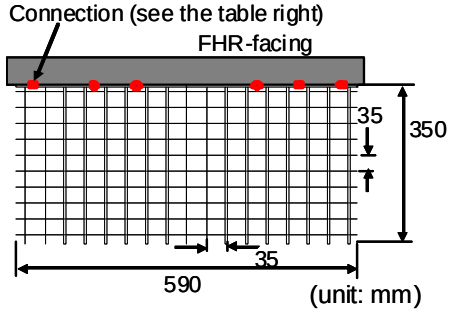

Fig. 40 Model reinforcement

(3 mm-thick, 50 mm-wide and 200 mm-long). The peak resisting moment of the fixture is about 0.5 kN-m, which is much smaller, by a factor of about 1/3, than the moment produced by the earth pressure activated on the back of the facing when the model failed. Twenty sinusoidal waves at a frequency of 5 Hz were applied at the shaking table step by step increasing the maximum acceleration, α_b, by an increment of 100 gal. A frequency of 5 Hz was chosen so that the applied load waves become detrimental to the models as actual severe earthquakes to prototype structures.

Figure 41 shows the residual settlements at 5 cm back of the facing on the crest of the backfill. With the GRS RW bridge, the settlement of the sill beam is presented. Figure 42 shows the residual lateral displacements at the top and bottom of the facing. Figure 43 shows the residual overturning angle of the facing, where the rotational angle of the sill beams of the GRS RW bridge is also presented. In these figures, with the traditional type bridge and the GRS RW bridge, the displacements of the abutment and the backfill on the side supporting the girder via a fixed shoe, where all the lateral inertial force of the girder is activated, are presented. Figure 44 shows the failure modes of the integral bridge and the GRS integral bridge observed after the respective tests. The following trends of behaviour may be seen from these figures:

(1) The GRS integral bridge is most stable among the four types, while the traditional type bridge is least stable.

(2) The stabilities of the GRS-RW bridge and integral bridge are similar and intermediate, although their failure modes are quite different. With the GRS-RW bridge, the GRS RWs themselves are very stable, whereas the stability of the sill beam that supports the girder via a fixed shoe is quite low.

(3) The basic failure modes of the integral and GRS integral bridges are the same: *i.e.*, pushing out of the facing bottom associated with rotation of the facing relative to the backfill (Fig. 44). The strength of the fixture integrating the girder and the facings is utterly insufficient to fully resist against this mode of facing displacement.

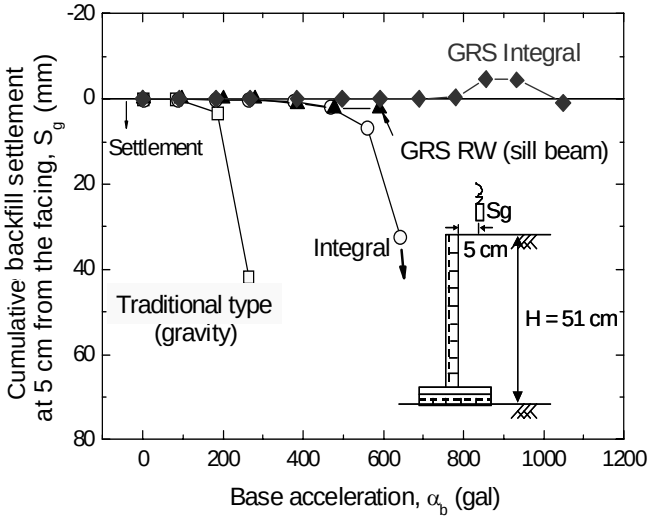

Fig. 41 Residual backfill settlement at 5 cm back of the facing plotted against base acceleration

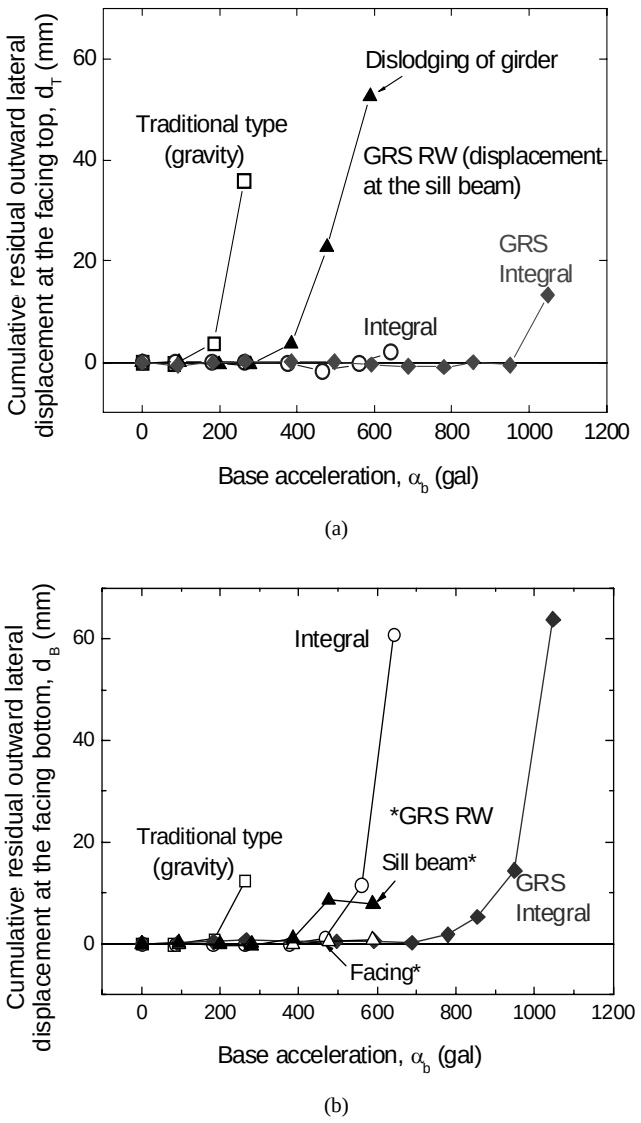

Fig. 42 Residual outward displacement at: (a) top; and (b) bottom of the facing, plotted against base acceleration

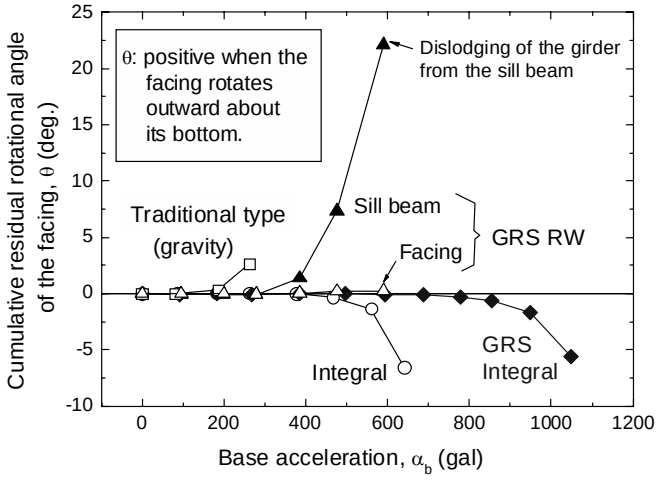

Fig. 43 Residual facing rotation plotted against base acceleration

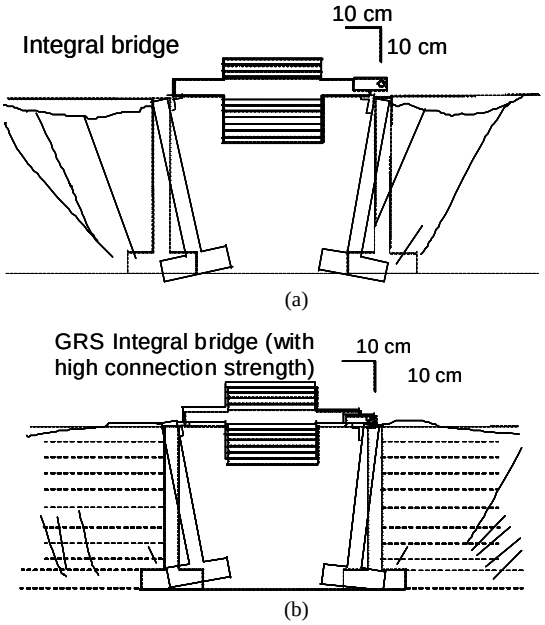

Fig. 44 Failure modes

Figure 45 shows the distributions with depth of earth pressure at the 10th cycle at different shaking stages activated on the back of the facing of the GRS integral bridge. In the upper part of the facing (*i.e.*, z < about 30 cm), the largest earth pressure in each cycle is activated when the facing top is under the passive condition, developed by the pushing-in movement of the girder into the backfill. On the other hand, in the lowest part of the facing (*i.e.*, z > about 30 cm), the largest earth pressure is activated when the footing bottom is moving toward the backfill. In Fig. 45(a), the earth pressure suddenly decreases when the base acceleration increases from 950 gals to 1,185 gals. This change is due to the start of significant rotational failure about the facing top in the backfill as shown in Fig. 44(b). These trends show that the major failure mode of the GRS integral bridge and integral bridge is the rotation of the facing relative to the backfill with the facing bottom being pushed out. This failure mode can also be detected from Fig. 46, which shows the maximum tensile strains in the reinforcement at respective shaking stages in the GRS integral bridge model. All these test results indicate that high connection strength between the reinforcement and the facing is essential for a high seismic stability of GRS integral bridge.

Figure 47 summarizes the load (L) and resistance (R) components for the facing rotation relative to the backfill for the GRS integral bridge, derived from the test results presented above. The two major resisting components are the passive pressure in the upper part of the backfill and the tensile force of the reinforcement at the lower part of the facing. The former can be increased by lightly cement-mixing relevant upper part of the backfill. The latter is the minimum value among the connection strength, the tensile rupture strength and the pull-out strength of the reinforcement. All these three components should be made sufficiently high.

More details on the study on the GRS integral bridge are described in Tatsuoka *et al*. (2008c).

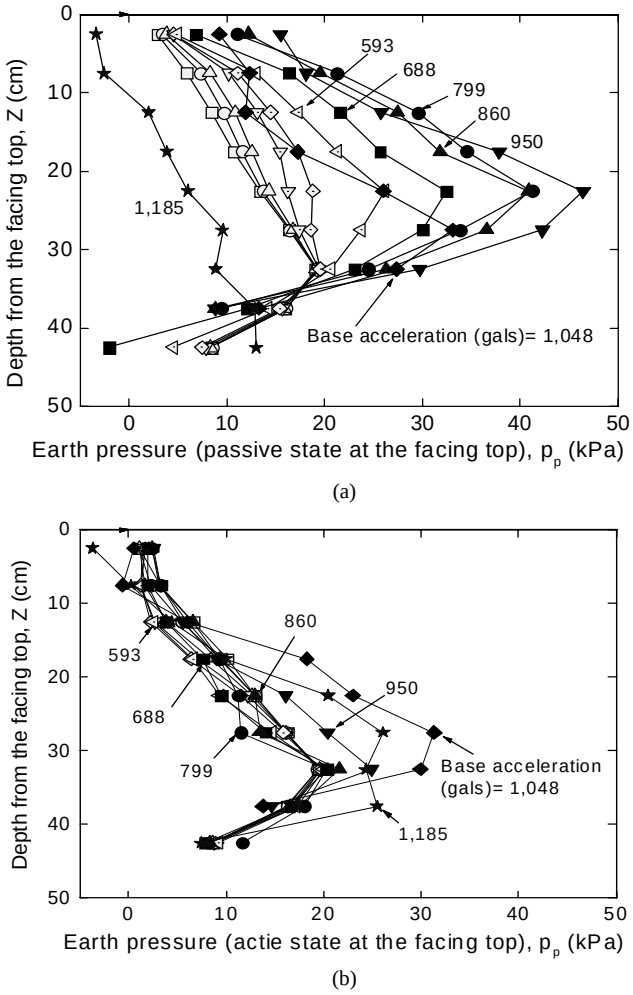

Fig. 45 Earth pressure on the facing at 10th cycle at each shaking stage, GRS integral bridge when the facing top is at: (a) passive state; and (b) active state

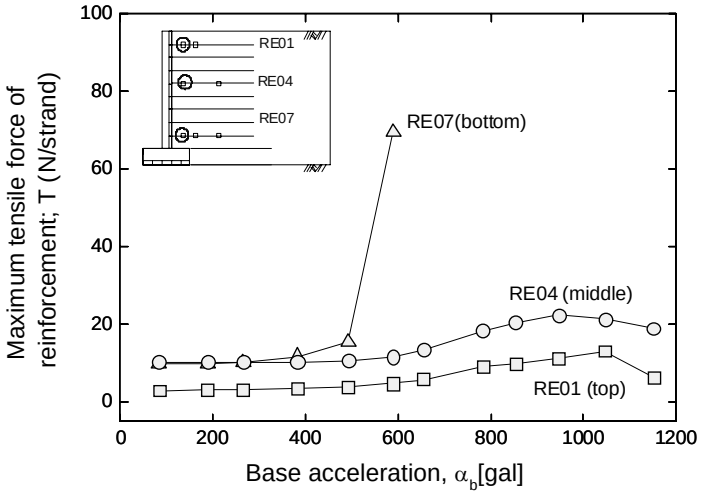

Fig. 46 Relationship between maximum tensile force of reinforcement and base acceleration, GRS integral bridge

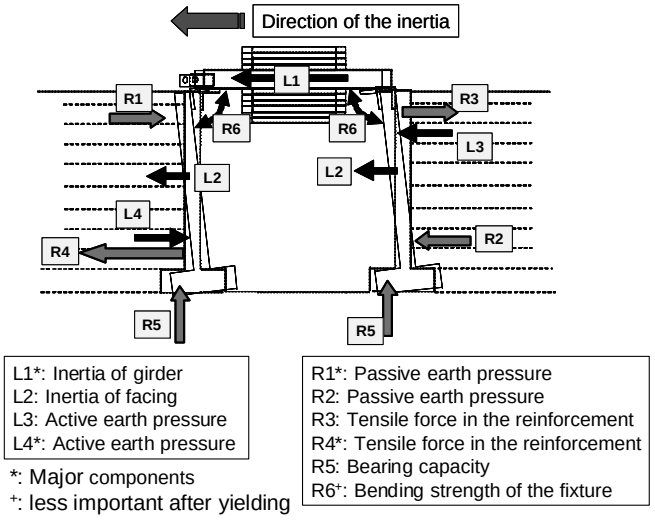

Fig. 47 Load and resistance components for the facing rotation relative to the backfill, GRS integral bridge

7. CONCLUSIONS

Geosynthetic-reinforced soil retaining walls (GRS RWs) having a stage-constructed full-height rigid (FHR) facing have been constructed as important permanent RWs for a total length of more than 100 km in Japan since 1999 until today (August 2008). Although these GRS RWs are mainly for railways, many others were also constructed for highways and other types of infrastructure. Its current popular use is due to not only high cost-effectiveness, but also high performance that is equivalent to, or even better than, other modern RWs. This success can be attributed to;

(1) the use of a proper type of reinforcement (*i.e.*, a geogrid for cohesionless soil and a nonwoven/woven geotextile composite for high-water content cohesive soil);

(2) casting-in-place of a FHR facing by staged construction procedures in such that reinforcement layers are firmly connected to the facing; and

(3) taking advantages of the rigidity of the facing in design.

Many embankments and traditional type RWs that collapsed during recent severe earthquakes and heavy rainfalls in Japan were reconstructed to embankments with steep geosynthetic-reinforced slopes or GRS RWs with a stage-constructed FHR facing or their combination. It was validated that this technology is highly cost-effective in not only reconstructing collapsed soil structures but also rehabilitating old soil structures.

A case history of high geosynthetic-reinforced soil walls showed significant importance of high compaction of the backfill to achieve very small residual deformation of the wall after wall completion. Analysis of the time histories of measured geogrid strains based on an elasto-viscoplastic theory showed that the tensile load in the geogrid decreases with time and, therefore, creep failure of the geogrid by the end of a specified life time is utterly unlikely.

A new bridge type, called the GRS integral bridge, is proposed, which comprises an integral bridge and geosynthetic-reinforced backfill. A series of static and dynamic loading model

tests showed that GRS integral bridges exhibit essentially zero settlement in the backfill and no structural damage to the facing when subjected to lateral cyclic displacements of the facing caused by seasonal thermal expansion and contraction of the girder, while their seismic stability is very high. Comparisons of the behaviour of GRS integral bridge with those of other three conventional bridge types showed that these features and high cost-effectiveness of the GSR integral bridge are due to that:

(1) shoes are not used;

(2) the girder is continuous without any connections;

(3) the backfill is reinforced with geogrid layers firmly connected to the facing; and

(4) FHR facings are stage-constructed after the construction of full-height geosynthetic-reinforced soil walls and then pile foundations (if necessary).

ACKNOWLEDGEMENTS

This paper is based on a long-term research more than 25 years performed by the author and his colleagues. The author sincerely appreciates all helps and efforts of his previous and current colleagues at University of Tokyo and Tokyo University of Science in performing this long-term research. The support of Dr. Tateyama, M. and his colleagues at the Railway Technical Research Institute, Japan, is highly appreciated.

REFERENCES

Aizawa, H., Nojiri, M., Hirakawa, D., Nishikiori, H., Tatsuoka, F., Tateyama, M. and Watanabe, K. (2007). "Validation of high seismic stability of a new type integral bridge consisting of geosynthetic-reinforced soil walls." *Proc. 5th Int. Sym. on Earth Reinforcement* (IS Kyushu 2007), Ochiai *et al*. eds., 819–825.

England, G, L., Neil, C, M. and Bush, D, I. (2000). *Integral Bridges, A Fundamental Approach to the Time-Temperature Loading Problem*, Thomas Telford.

Fujita, Y., Sugimoto, T., Nakamura, Y., Kawahata, S., Funada, H., Yoshida, T., Ito, M. and Yoshida, K. (2008). "High geogrid-reinforced retaining walls for a new air-port." *Proc. 4th Geo-Synthetics Asia*, Shanghai.

Hirakawa, D., Nojiri, M., Aizawa, H., Tatsuoka, F., Sumiyoshi, T. and Uchimura, T. (2006). "Behaviour of geosynthetic-reinforced soil retaining wall subjected to forced cyclic horizontal displacement at wall face." *Proc. 8th Int. Conf. on Geosynthetics*, Yokohama, 1075–1078.

Hirakawa, D., Nojiri, M., Aizawa, H., Tatsuoka, F., Sumiyoshi, T. and Uchimura, T. (2007(a)). "Residual earth pressure on a retaining wall with sand backfill subjected to forced cyclic lateral displacements." *Soil Stress-Strain Behavior: Measurement, Modeling and Analysis, Geotech. Symposium*, Roma, Ling *et al*., eds., 865–874.

Hirakawa, D., Nojiri, M., Aizawa, H., Nishikiori, H., Tatsuoka, F., Tateyama, M. and Watanabe, K. (2007b). "Effects of the tensile resistance of reinforcement embedded in the backfill on the seismic stability of GRS integral bridge." *Proc. 5th Int. Sym. on Earth Reinforcement*, Ochiai *et al*. eds., IS Kyushu, 811–817.

Kongkitkul, W., Hirakawa, D., Sugimoto, T., Kawahata, S., Yoshida, T., Ito, S. and Tatsuoka, F. (2008). "Post-construction time history of tensile force in the geogrid arranged in a full-scale high wall." *Proc. 4th GeoSynthetics Asia*, Shanghai, 64-69.

Koseki, J., Bathurst, R. J., Guler, E., Kuwano, J. and Maugeri, M. (2006). "Seismic stability of reinforced soil walls." *Proc. 8th International Conference on Geosynthetics*, Yokohama, **1**, 51–77.

Koseki, J., Tateyama, M., Watanabe, K. and Nakajima, S. (2008). "Stability of earth structures against high seismic loads." *Keynote Lecture, Proc. 13th ARC on SMGE*, Kolkata, II.

Morishima, H., Saruya, K. and Aizawa, F. (2005). "Damage to soils structures of railway and their reconstruction." *Special Issue on Lessons from the 2004 Niigata-ken Chu-Etsu Earthquake and Reconstruction, Foundation Engineering and Equipment (Kiso-ko)*, October, 78–83 (in Japanese).

Maruyama, N., Murayama, M., and Sasaki, F. (2006). "Construction of a geogrid-reinforced counter-weight fill to increase the seismic stability of an existing earth dam." *Proc. 8th International Conference on Geosynthetics*, Yokohama, 643–646.

Masuda, T., Tatsuoka, F., Yamada, S. and Sato, T. (1999). "Stress-strain behaviour of sand in plane strain compression, extension and cyclic loading tests." *Soils and Foundations*, **39**(5), 31–45.

Nakarai, K., Uchimura, T., Tatsuoka, F., Shinoda, M., Watanabe, K. and Tateyama, M. (2002). "Seismic stability of geosynthetic-reinforced soil bridge abutment." *Proc. 7th Int. Conf. on Geosynthetics*, Nice, **1**, 249–252.

Ng, C., Springman, S. and Norrish, A. (1998). "Soil-structure interaction of spread-base integral bridge abutments." *Soils and Foundations*, **38**(1), 145–162.

Shinoda, M., Uchimura, T. and Tatsuoka, F. (2003a). "Increasing the stiffness of mechanically reinforced backfill by preloading and prestressing." *Soils and Foundations*, **43**(1), 75–92.

Shinoda, M., Uchimura, T and Tatsuoka, F. (2003b). "Improving the dynamic performance of preloaded and prestressed mechanically reinforced backfill by using a ratchet connection." *Soils and Foundations*, **43**(2), 33–54.

Soma, R., Sonoda, Y., Aizawa, H., Nishikiori, H., Tatsuoka, F. and Hirakawa, D. (2008). "Effects of cement-stabilization of the backfill on seismic performance of GRS integral bridge." *Proc. 43rd Japanese National Conference on Geotechnical Engineering, Hiroshima* (in Japanese).

Tamura, Y., Nakamura, K., Tateyama, M., Murata, O., Tatsuoka, F. and Nakaya, T. (1994). "Full-scale lateral loading tests of column foundations in geosynthetic-reinforced soil retaining walls." *Proc. of Int. Symposium Recent Case Histories of Permanent Geosynthetic-Reinforced Soil Retaining Walls*, Tatsuoka and Leshchinsky eds., Balkema, 277–286.

Tateyama, M., Murata, O., Tamura, Y., Tatsuoka, F. and Nakaya, T. (1994). "Lateral loading tests on columns on the facing of geosynthetic-reinforced soil retaining wall." *Proc. of Int. Symposium Recent Case Histories of Permanent Geosynthetic-Reinforced Soil Retaining Walls*, Tatsuoka and Leshchinsky eds., Balkema, 287–294.

Tatsuoka, F. (1992). "Roles of facing rigidity in soil reinforcing." *Keynote Lecture, Proc. Earth Reinforcement Practice, IS-Kyushu '92*, Ochiai *et al*. eds., **2**, 831–870.

Tatsuoka, F., Tateyama, M, Uchimura, T. and Koseki, J. (1997). "Geosynthetic-reinforced soil retaining walls as important permanent structures." *Geosynthetic International*, **4**(2), 81–136.

Tatsuoka, F., Koseki, J., Tateyama, M., Munaf, Y. and Horii, N. (1998). "Seismic stability against high seismic loads of geosynthetic-reinforced soil retaining structures." *Keynote Lecture*, 99*Proc. 6th Int. Conf. on Geosynthetics*, Atlanta, **1**, 103–142.

Tatsuoka, F., Masuda, T. and Siddiquee, M. S. A. (2003). "Modelling the stress-strain behaviour of sand in cyclic plane strain loading, geotechnical and environmental engineering." *Journal of Geotechnical and Environmental Engineering, ASCE*, **129**(6), 450–467.

Tatsuoka, F. (2004). "Cement-mixed soil for trans-tokyo bay highway and railway bridge abutments, geotechnical engineering for transportation projects." *Proc. GeoTrans 04*, Los Angels, ASCE GSP 126, Yegian and Kavazanjian eds., 18–76.

Tatsuoka, F., Hirakawa, D., Shinoda, M., Kongkitkul, W. and Uchimura, T. (2004). "An old but new issue; viscous properties of polymer geosynthetic reinforcement and geosynthetic-reinforced soil structures." *Keynote Lecture, Proc. GeoAsia04*, Seoul, 29–77.

Tatsuoka, F., Tateyama, M., Aoki, H. and Watanabe, K. (2005). "Bridge abutment made of cement-mixed gravel backfill." *Ground Improvement, Case Histories, Elsevier GeoEngineering Book Series*, **3**, Indradratna and Chu eds., 829–873.

Tatsuoka, F., Kongkitkul, W. and Hirakawa, D. (2006). "Viscous property and time-dependent degradation of geosynthetic reinforcement." *Proc. 8th Int. Conf. on Geosynthetics*, Yokohama, **4**, 1587–1590.

Tatsuoka, F., Tateyama, M., Mohri, Y. and Matsushima, K. (2007a). "Remedial treatment of soil structures using geosynthetic-reinforcing technology." *Geotextiles and Geomembranes*, **25**(4) and (5), 204–220.

Tatsuoka, F., Hirakawa, D., Nojiri, M. and Aizawa, H., Tateyama, M. and Watanabe, K. (2007b). "A new type integral bridge comprising geosynthetic-reinforced soil walls." *Proc. 5th Int. Sym. on Earth Reinforcement*, Ochiai *et al*., eds., IS Kyushu, 803–809.

Tatsuoka, F., Hirakawa, D., Nojiri, M., Aizawa, H., Tateyama, M. and Watanabe, K. (2008a). "Integral bridge with geosynthetic-reinforced backfill." *Proc. First Pan American Geosynthetics Conference and Exhibition*, Cancun, Mexico, 1199–1208.

Tatsuoka, F., Hirakawa, D., Aizawa, H. Nishikiori, H. Soma, R and Sonoda, Y. (2008b). "Importance of strong connection between geosynthetic reinforcement and facing for GRS integral bridge." *Proc. 4th GeoSynthetics Asia*, Shanghai, 205-210.

Tatsuoka, F. (2008). "Geosynthetics Engineering, combining two engineering disciplines." *Special Lecture, Proc. GeoSynthetics Asia*, Shanghai, 1-35.

Tatsuoka, F., Hirakawa, D., Nojiri, M., Aizawa, H., Nishikiori, H., Soma, R., Tateyama, M. and Watanabe, K. (2008c). A New type integral bridge comprising geosynthetic-reinforced soil walls, *Geotextiles and Geomembranes* (accepted for publication).

Uchimura, T., Tateyama, M., Koga, T. and Tatsuoka, F. (2003a). "Performance of a preloaded-prestressed geogrid-reinforced soil pier for a railway bridge." *Soils and Foundations*, **43**(6), 33–50.

Uchimura, T., Tatsuoka, F. and Nakarai, K. (2003b). Seismic stability of preloaded and prestressed reinforced soil abutments, *Proc. 12th Asian Regional Conference on Soil Mechanics and Foundation Engineering*, Singapore.

Uchimura, T., Tamura, Y., Tateyama, M., Tanaka, I., and Tatsuoka, F. (2005). "Vertical and horizontal loading tests on full-scale preloaded and prestressed geogrid-reinforced soil structures." *Soils and Foundations*, **45**(6), 65–74.

Watanabe, K., Tateyama, M., Yonezawa, T., Aoki, H., Tatsuoka, F. and Koseki, J. (2002). "Shaking table tests on a new type bridge abutment with geogrid-reinforced cement treated backfill." *Proc. 7th Int. Conf. on Geosynthetics*, Nice, **1**, 119–122.